Microcapsule Drug Delivery Device for Treatment of Glioblastoma Multiforme

by

Alexander Wesley Scott

B.S. Materials Science and Engineering, Virginia Polytechnic Institute and State University (2007)

Submitted to the Department of Materials Science and Engineering in partial fulfillment of the requirements for the degree of

Master of Science in Materials Science and Engineering

at the

MASSACHUSETTS INSTITUTE OF TECHNOLOGY

June 2010

Author .....
Department of Materials Science and Engineering
May 6, 2010

Certified by .....
Michael J. Cima, Ph.D.
Professor
Thesis Supervisor

Certified by .....
Robert S. Langer, Sc.D.
Institute Professor
Thesis Supervisor

Accepted by .....
Christine Ortiz
Chair, Departmental Committee on Graduate Students

Microcapsule Drug Delivery Device for Treatment of Glioblastoma Multiforme

by

Alexander Wesley Scott

Submitted to the Department of Materials Science and Engineering
on May 6, 2010, in partial fulfillment of the
requirements for the degree of
Master of Science in Materials Science and Engineering

Abstract

Controlled-release drug delivery systems are capable of treating debilitating diseases, including cancer. Brain cancer, in particular glioblastoma multiforme (GBM), is an extremely invasive cancer with a dismal prognosis. The use of drugs capable of crossing the blood-brain barrier has shown modest prolongation in patient survival, but not without unsatisfactory systemic, dose-limiting toxicity. Localized delivery of potent chemotherapeutics aims to lower systemic toxicity while increasing drug concentrations directly to the tumor site. I have developed implantable drug delivery microcapsule devices for the localized delivery of temozolomide and for treatment of glioblastoma multiforme in this work. I have been able to modulate the drug release profiles from these microcapsules based on the physical chemistry of the drug and the dimensions of the release orifices in these devices. Experimental *in vitro* studies were performed in order to test the function, reliability, and drug release kinetics of the devices. The experimental release curves showed mass flow rates of 36 ug/hr for single-orifice devices and an 88 ug/hr mass flow rate for multiple-orifice devices loaded with temozolomide. Intracranial temozolomide-filled microcapsules were tested in a rodent 9L glioma model. Outcomes were animal survival and immunohistochemical analysis of tissue for evidence of DNA strand breaks via terminal deoxynucleotidyl transferase dUTP nick end labeling (TUNEL) assay. Results showed that localized delivery of chemotherapeutics from microcapsule devices is capable of prolonging animal survival and may offer an alternative to the harsh side-effects and low response rates inherent to systemic drug administration in GBM patients.

Thesis Supervisor: Michael J. Cima, Ph.D.
Title: Professor

Thesis Supervisor: Robert S. Langer, Sc.D.
Title: Institute Professor

Acknowledgments

I would like to thank my advisors, Michael Cima and Robert Langer, for their help and guidance with the work conducted in this thesis.

I would also like to thank my wonderful labmates (especially Yoda, Byron, Urvashi, and all the folks at Johns Hopkins) for their excellent insights, helpful criticism, and delicious dinners.

Big shout out to all my "awesom-o" and PPST fam here at MIT, you all made MIT tolerable (and even enjoyable at times).

Thank you to Liz and my labmates for reviewing the many drafts of this thesis.

Last but not least, thanks to my Mother (Diane), Father (Curtis), Sister (Kristen), Brother (Taylor), and Brother-in-Law (Taison) for their support during the trying times at MIT.

And with that...LETS GO!

Contents

List of Figures

List of Tables

Chapter 1

Background

1.1 Introduction

The broad motivation of this work is to design and develop a polymeric, diffusion-based drug delivery microcapsule for localized treatment of human disease. This thesis discusses the more specific aim of designing such devices for treatment of glioblastoma multiforme (GBM), a debilitating form of brain cancer. An understanding of both GBM biology and the current state-of-the-art in GBM tumor maintenance and treatment will help to determine drug delivery methods with high clinical relevance that will guide the design of these devices.

The chemotherapeutic drugs of interest to this project are temozolomide (TMZ) and doxorubicin hydrochloride (DOX). Studies detailing the physical chemistry of these drugs, along with the engineering principles of small molecule diffusion, will allow for the fabrication of drug delivery devices that can deliver virtually any drug formulation over a chosen period of time. Liquid crystal polymer (LCP) and poly(L)lactic acid (PLLA) polymers will serve as the housing and vehicle for drug release. *In vitro* drug release studies will be performed in order to test the function, reliability, and drug release kinetics of the devices prior to *in vivo* efficacy studies that will be performed in an intracranial rodent model of GBM. The results of these experiments will shed light on the feasibility of treating GBM through localized delivery of chemotherapeutic agents.

1.2 Glioblastoma Multiforme

1.2.1 Classification

Tumors of the central nervous system (CNS) represent a group of neoplasms that have a wide range of genetic heterogeneity, are extremely difficult to classify, and currently have no curative options. The World Health Organization (WHO) classifies tumors of the CNS into nine categories according to the cell of tumor origin [1]. The classification of astrocytic tumors includes the degree of tumor "aggressiveness." Relatively slower-growing astrocytic tumors are termed "low-grade" tumors, whereas more rapidly-growing tumors are "high-grade." Tumor progression from low to high-grade status is associated with increased mitotic index, vascular endothelial proliferation, and necrosis [2]. High-grade astrocytic tumors most commonly include anaplastic (undifferentiated) astrocytomas (AA) and glioblastoma multiforme (GBM). These tumors are also referred to as malignant gliomas due to their biological classification as glial cells. GBM diagnosis is associated with the worst prognosis of all brain tumors and is the focus of the work performed in this thesis.

The World Health Organization further categorizes astrocytic tumors into four classes, or grades, with GBM being the most invasive and malignant type (grade IV). Tumors of the other three grades are pilocytic astrocytomas (grade I), astrocytomas (grade II), and anaplastic astrocytomas (grade III) [3]. GBM is the most frequent primary malignant brain tumor, accounting for 12-15% of all brain tumors, and 60-75% of astrocytic tumors [4]. The prevalence of GBM in the Western hemisphere is about 3-4/100,000 new cases per year [4]. GBM occurs in patients of all ages, races, and genders but is more common among Caucasians. Men have a higher GBM mortality rate than women by a ratio of (3:2) [5][1]. GBM occurrence is rare below the age of 40 and is most prevalent in the later years of life with a peak at 50 years of age [5]. Pediatric patients are also more susceptible to development of malignant GBM than younger adult patients, and occurrence rates plateau in people over 70 years of age [1].

The relatively high prevalence of GBM among brain tumor patients is unfortu-

nate due to the dismal prognosis that accompanies these neoplasms. Median patient survival is estimated to be between 12 and 18 months when patients receive maximal treatment. This treatment includes surgical resection, radiation treatment, and usually chemotherapy [6]. There have been few reports of complete GBM regression; the overall 5-year survival rate is less than 10%, and the final mortality rate for all patients is close to 100% [6]. The need for novel treatment strategies for primary and recurrent GBM is crucial to the lives of these patients.

1.2.2 Natural History

Recent research has focused on the hypothesis that GBM tumor masses contain a sub-population of cells with heterogenous genotypic and phenotypic traits. This heterogeneity is due to the complex genetic alterations that occur during GBM formation from properly-functioning astrocytes. Inactivation of tumor suppressor genes along with oncogene activation and overexpression are common traits in malignant glioma [1]. A proposed schematic of the genetic pathways involved in astrocyte-to-GBM transformation is shown in Figure 1-1[2]. Figure 1-1 shows that genetic mutations

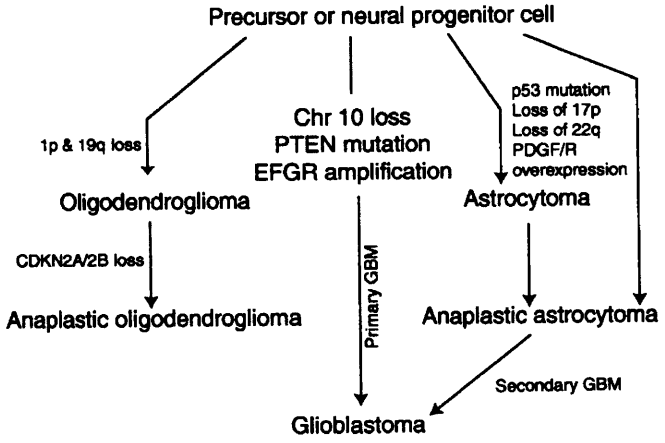

Figure 1-1: GBM development pathway
[2]

cause formation of malignant gliomas, and it has been hypothesized that an even larger number of genes may be involved. Mutations in the genetic profile of GBM cells also contribute to their chemotherapeutic resistance by inducing alterations in

genes that protect against cell death [2]. The expression of multi-drug resistance genes (MDR) and 06-methylguanine-methyltransferase (MGMT) are associated with the expression of chemoresistance phenotypes [2].

Genetic mutations in GBM induce the overexpression of specific growth factors that facilitate the formation of new blood vessels through the process of angiogenesis. Fibroblast growth factor (FGF) and vascular endothelial growth factor (VEGF) are two common mediators of angiogenesis [1]. Glioma cells are able to increase their oxygen and nutrient supply by forming new blood vessels, which facilitate a greater chance of tumor cell survival. Drugs such as Avastin are being investigated for their ability of block VEGF and stop the production of blood vessels.

The high mortality rate associated with GBM is also attributed to a multitude of physical properties that are unique to these gliomas. The most significant of these properties is the unsatisfactory spatial location and orientation of the malignancy. GBM occurs most frequently in the frontal and temporal lobes of the brain but can often invade the basal ganglia and brain stem [5]. GBM may also appear in the central part of the brain with a characteristic "butterfly" pattern that occupies the corpus callosum and extends bilaterally into the centrum semiovale of both hemispheres [5].

The invasive nature of GBM is problematic. Research has suggested that gliomas are capable of moving throughout the brain through chemical modulation of the surrounding extracellular matrix (ECM). The processes through which tumor cells are able to control such migration is not fully understood, but the migration is thought to occur through the secretion of metalloproteases that cause degradation of the ECM[1]. Surgical resection has been shown to improve patient survival[2], but GBM commonly spreads to invade eloquent areas of the brain where surgeons are unable to operate because such operations would substantially decrease neurological function and patient quality-of-life (QOL). This spreading results in minimal surgical debulking, which in turn leaves a substantial amount of tumor mass unaddressed. The residual tumor cells are then able to migrate throughout the brain tissue, causing the high incidence of GBM recurrence. Surgical intervention is even more difficult when the GBM tumor mass contains diffuse, ill-defined physical boundaries[5].

1.2.3 Tumor Recurrence

Recurrence of GBM following surgical resection contributes substantially to the unfavorable prognosis associated with these malignancies. Despite extensive surgical intervention, GBM recurrence is inevitable after a median patient survival time of 32 to 36 weeks, and it has been reported that 90% of patients with glioma will experience tumor recurrence near the original tumor location [6][6]. Not all tumors recur at the original tumor site. Studies have shown that the most common site of GBM recurrence is 2 to 3 cm from the border of the original lesion[6].

Treatment strategies for recurrent GBM are confounded by the lack of uniform definition and criteria of recurrent GBM, institutional variability in treatment, and the heterogenous nature of recurrence in terms of glioma spatial location and acquired resistance to chemotherapy. Researchers and clinicians usually define GBM recurrence as a change from a previous interval of tumor absence or a loss of prior complete tumor control [6]. These requirements are too vague, and a more definite set of criteria need to be established in order to treat patients in a consistent manner. It would otherwise not be possible to compare clinical trials from different institutions without substantial doubt as to what form of GBM (primary or recurrent) is being examined.

1.3 Treatment Options

1.3.1 Surgical Resection

The treatment of GBM has classically included surgery followed by radiation therapy. Surgical intervention is crucial because it provides clinicians with tissue samples that are used to confirm the histological status and malignancy of the tumor. This allows for a more robust diagnosis than that obtained by most imaging techniques [6]. The extent of surgical resection has been proven to be an important prognostic factor in treating GBM patients. A retrospective analysis by the Montreal Neurological Institute showed that patients who had complete surgical resection had a better overall

prognosis that those with incomplete tumor resection [7]. Surgery can also confirm tumor recurrence, reduce intracranial pressure and mass effect, improve patients' neurological status, and improve efficacy of adjunctive therapy [1] [6]. Controversy between institutions exists about the absolute degree of tumor resection that will meaningfully change outcome, but it is widely accepted that even minimal surgical intervention should be performed whenever possible.

1.3.2 Radiation

Whole-brain and localized radiation treatment is usually carried out with x-rays produced by linear accelerators. Three-dimensional imaging techniques are commonly used for localized radiation treatment. Localized treatment is especially beneficial for patients whose tumor mass is located in operable locations or if the lesion is relatively small. Radiation dosage is limited by the tissue tolerance of normal white brain matter, and a cumulative dose of 60 Gy[1] is usually given over a prescribed time period. Radiation-induced tissue necrosis is the primary side-effect and limiter to radiation treatment.

Interstitial brachytherapy and gamma knife radiosurgery are two of the most common types of localized radiation treatment for GBM. Stereotactic surgical procedures allow for the placement of either removable or permanent Iodine-125 interstitial brachytherapy radiation sources. Permanent interstitial sources have been found to be safer than removable sources due to the high incidence of late-term radiation injury from removable sources [1]. Studies have reported a median survival time of 9.1 months in patients with recurrent GBM when brachytherapy was used. A 3-year survival rate of 15% was also achieved against recurrent GBM treated with high-activity Iodine-125 radio sources [6]. Infection, edema, radiation toxicity, and tissue necrosis are the primary risks associated with interstitial brachytherapy.

Gamma knife radiosurgery is especially useful in addressing small lesions with unsatisfactory spatial orientation in the brain. Radiosurgery is a non-invasive technique that typically requires placement of the skull in a stereotaxic frame. It allows multiple radiation source beams to converge on a small target GBM lesion to produce

localized irradiation [1]. The Gamma Knife radiosurgery system by AB Elekta and modified linear accelerators have been used as radiosurgery instruments. Risks to the patient are similar to those of interstitial brachytherapy; local radiation-induced tissue necrosis is the most common and damaging side-effect.

1.3.3 Chemotherapy

Chemotherapy is a versatile treatment strategy that allows for the development of novel therapies against malignant gliomas. Chemotherapeutic agents are commonly administered following surgical resection and irradiation of GBM lesions. Drugs may be given systemically or directly to the tumor bed. Some chemotherapeutics act as "radiosensitizers" that enhance the effect of radiation therapy and are given concomitantly with radiation treatment.

A range of chemotherapeutic drugs have been investigated for action against GBM *in vitro* and *in vivo*. A sample list of these drugs is given in Table 1-1. The three main cytotoxic mechanisms through which chemotherapeutic drugs act are DNA damage, DNA replication inhibition, and cytoskeletal disruption. An extensive review of each of the chemotherapies presented in Table 1-1 is beyond the scope of this thesis, and the discussion will instead focus on the drugs that are most clinically relevant to current GBM treatment. The drugs used in this work are temozolomide (TMZ) and doxorubicin hydrochloride (DOX). Carmustine (BCNU) will also be discussed due to its historical importance as a chemotherapeutic agent against GBM and its use in the development of novel drug delivery strategies. The cytotoxic mechanisms of BCNU, TMZ, and DOX have been studied extensively and will be briefly discussed in the following sections. Satisfactory delivery of these agents (systemic vs. localized treatment) is of the utmost concern in treating GBM and is the underlying motivation for the research and development of the drug delivery microcapsules described in this thesis.

DNA damaging agents	DNA replication inhibitors
Nitrosoureas	*Topoisomerase inhibitors*
Carmustine (BNCU)	Etoposide
Lomustine (CCNU)	Teniposide
Nimustine (ACNU)	Topotecan
Semustine (MeCCNU)	*Antimetabolites*
PCNU	Methotraxate (MTX)
Platinum compounds	5-Fluorouracil (5-FU)
Cisplatin (CDDP)	Cytarabine (Ara-C)
Carboplatin	5-Fluorocytosine (5-FC)
Nitrogen mustards	6-Tioguanine
Cyclophosphamide (CPA)	Iododeoxyuridine
Melphalan	Methylprednisolone
Ifosfamide	Bromodeoxyuridine
Mafosphamide	**Cytoskeletal disrupting agents**
Antibiotics	*Vinca alkaloids*
Bleomycin	Vinblastine
Doxorubicin	Vincristine
Actinomycin D	*Taxenes*
Aziridinylbenzoquinon (AZQ)	Paclitaxel
Epirubicin	Docetaxel
Others	**Miscellaneous agents**
Temozolomide	Tamoxifen
Procarbazine	Bryostatin
Dacarbazine	7-Hydroxystaurosporine (UCN-01)
Thiopeta	Leflunomide (SU-101)
Chlorambucil	Mitoxantrone
Busulfan	Lovastatin
Spirohydantoin mustard (SHM)	

Table 1.1: Chemotherapeutic Drugs used for Treatment of GBM [2]

Carmustine

Carmustine (BCNU) (1-3-bis(2-chloroethyl)-1-nitrosourea) had historically been the focus of major study as it was one of the first chemotherapeutic drugs approved for brain tumor treatment [8]. Initial clinical trials of BCNU against brain tumors began in 1964, and FDA approval was granted in March 1977. Clinical trials also showed that BCNU administration produced a survival advantage of an additional 2 months when compared with radiation therapy alone [8].

The primary cytotoxic mechanism induced by BCNU is the cross-linking of DNA strands by chloroethylation of DNA at a nucleophilic site on one DNA strand and displacement of a chloride ion on the other strand [9] [10]. Chloroethylation produces ethyl bridges between these two DNA strands. This cross-linking causes the disruption of DNA unwinding that ultimately hinders synthesis of DNA and RNA.

Intravenous perfusion (IV) or oral administration are the traditional methods of delivering BCNU to the tumor site. The action of BCNU against gliomas is shown to be dose-dependent, with higher exposure resulting in decreased tumor growth in a rodent model of GBM [11]. Systemic delivery of BCNU has prolonged the survival of GBM patients but not without significant drawbacks such as debilitating side-effects, insufficient drug exposure due to the short half-life of BCNU, and unsatisfactory drug distribution throughout the brain[8].

Common side-effects caused by systemic administration of BCNU include hematopoietic depression, nausea and vomiting, acute leukemia, damaging cytotoxic effects on the kidney, liver, lungs, and central nervous system, and short drug exposure time to tumor tissue [10]. Life-threatening adverse events include severe brain edema and seizures[12]. The necessity of frequent repeat clinical visits for IV perfusion also makes systemic delivery of BCNU unattractive to patients. Studies have shown that BCNU tumor penetration and radial drug distribution are very low (2 mm) when delivered systemically [8]. Novel delivery methods to overcome toxic BCNU-induced side-effects and increase drug exposure to the tumor bed will be discussed in the following section.

Temozolomide

Temozolomide (TMZ) [13] is the current standard chemotherapeutic drug used for the treatment of GBM. The development of TMZ dates back to the early 1980s when the drug was first synthesized by scientists at Aston University. Temozolomide is categorized as a pro-drug due to the fact that its hydrolyzed product, MTIC, is the biologically active component of the drug. Once formed from TMZ, MTIC rapidly breaks down to form the highly reactive methyldiazonium ion [9]. The decomposition/hydrolysis mechanisms for TMZ are shown in Figure 1-2.

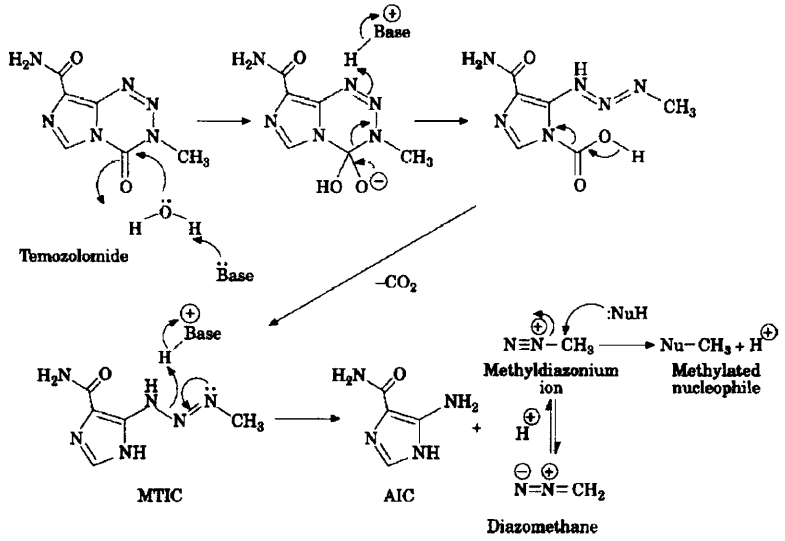

Figure 1-2: Temozolomide decomposition pathways [14]

The production of MTIC from TMZ in aqueous solution is highly dependent on the pH of the environment. Temozolomide is stable under acidic conditions, but the rate of degradation increases as the pH becomes more basic. In phosphate buffer at pH 7.4, the half-life of TMZ is 1.24h [14]. The MTIC molecule exhibits pH-dependent stability opposite to that of TMZ. MTIC is stable at basic pH and rapidly degrades in acidic environments.

The stability of TMZ in acidic conditions allows it to be administered orally because the TMZ molecule is able to withstand the high acidity of the stomach. After leaving the systemic circulation and passing through the blood brain barrier

(BBB), the pH of the surrounding environment changes. Brain tumors have a more alkaline pH than normal brain tissue [14]. This change in pH suggests that once TMZ reaches the intracranial tumor mass, pH-mediated decomposition of TMZ results in the formation of cytotoxic MTIC molecules.

The primary antitumor effect caused by TMZ is methylation of tumoral DNA [14]. The methylation process begins when the methyldiazonium ion formed from MTIC gives its methyl group to the guanine molecules in GBM DNA. This results in the formation of O^6- and N^7-methylguanine. DNA methylation by methyldiazonium also forms O^6-methylguanine, which is the primary cytotoxic methylation event. The formation of O^6-methylguanine in the DNA leads to base mismatch between two DNA strands. After DNA methylation by TMZ, DNA mismatch repair enzymes work to remove the non-complementary bases, which in turn generates single and double-strand breaks in the DNA helix. These breaks activate apoptotic pathways in the cell cycle that eventually lead to cell death.

The approved chemotherapeutic schedule for TMZ is currently a daily dose of 150 to 200 mg/m^2 for 5 days of every 28-day cycle[15]. Clinical trials during the development of TMZ lead to the discovery of its dose-limiting, toxic side-effects. When given orally, the primary dose-limiting hematologic side-effects associated with TMZ are leukopenia, seizure, thrombocytopenia, and myelosuppression [14]. Myelosuppression and seizure are usually the most serious side-effects and are controlled by reducing the TMZ dosing schedule or dosage. Non-hematologic side-effects include nausea, vomiting, fatigue, constipation, and headache [9].

Doxorubicin Hydrochloride

Doxorubicin (DOX) is an anthracycline antibiotic with strong antitumor action against lymphoblastic leukemias, sarcomas, lymphomas, mesotheliomas, carcinomas of the head and neck, and cancers of the breast, pancreas, stomach, liver, ovary, lung, and prostate [16]. Development of doxorubicin began in the 1950s when researchers began to search for tumoricidal compounds produced by soil-based microbes. The doxorubicin molecule is synthesized by the *Streptomyces peucetius* var. *caesius* fungus that

is found in Italy and is sometimes referred to as Adriamycin[17].

Doxorubicin causes cytotoxicity by intercalation within tumor cell DNA. The chemical structure of DOX is depicted in Figure 1-3, and sheds light on the drug's ability to disrupt the structure of cellular DNA helices [18]. The chemical structure

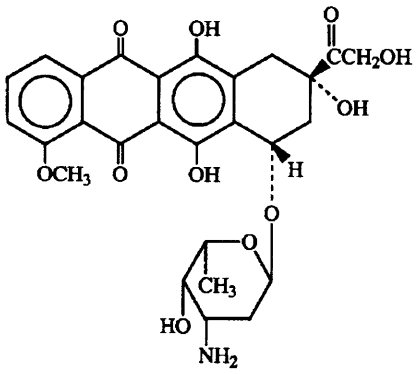

Figure 1-3: Doxorubicin chemical structure
[18]

of doxorubicin is predominantly a planar anthracycline ring. This allows for facile intercalation of doxorubicin into the DNA double helix and causes interference of DNA polymerases [18]. Doxorubicin also disrupts the progression of the topoisomerase II enzyme, which unwinds DNA during transcription. These two mechanisms both contribute to DNA, RNA, and protein synthesis inhibition and in turn arrest cell proliferation during the S-phase of the cell cycle.

Doxorubicin is typically administered as an IV infusion of 40-75 mg/m^2 dose. This dose is repeated at 3-4 week intervals until a cumulative dose of 450-550 mg/m^2 is reached. The risk of developing drug-related myocardial toxicity increases dramatically beyond this systemic dose. Congestive heart failure caused by doxorubicin exposure is estimated to be as high as 20% in patients who receive cumulative doses greater than 500 mg/m^2. The prevalence of congestive heart failure severely limits the usefulness of systemically-administered doxorubicin for treating GBM.

1.4 Barriers to Effective Chemotherapy

Extensive *in vitro* and *in vivo* studies have proven that BCNU, TMZ, and DOX are all able to induce cytotoxic DNA damage to GBM cells. The administration of chemotherapeutic molecules seldom results in long-term patient survival despite these chemotherapeutic agents' cytotoxic abilities and only extends survival by months at best. Low chemotherapeutic response rates are attributed to the presence of an intact BBB, unsatisfactory drug chemical stability (short half-life), harsh systemic side-effects (discussed earlier), development of genetic drug resistance mechanisms, low drug distribution profiles, and small drug payloads to the brain. All of these issues result in low tumor exposure to drug and contribute to unsatisfactory outcomes associated with chemotherapy. The goal of this thesis is to develop a drug delivery microcapsule that is capable of addressing each of these limitations in a clinically-relevant design.

1.4.1 Blood Brain Barrier (BBB)

The BBB is located at the capillary endothelium level of the brain, and its primary function is to act as a molecular filter that separates the systemically circulating blood from cerebrospinal fluid. The BBB is composed of tight junctions between capillary endothelial cells, membrane pumps, and the endothelial basal membrane[4]. These tight junctions restrict the diffusion of large, hydrophilic molecules while allowing the diffusion of small, hydrophobic (or lipophilic) molecules such as O_2. Harmful materials such as bacteria are actively blocked by the BBB, but the passage of nutrients and other small molecules that are necessary for brain cell survival is allowed.

The TMZ molecule is lipophilic and small, with a molecular weight of 194.151 daltons[19]. These two properties enable TMZ to pass through the blood-brain-barrier (BBB) very effectively after oral administration of the drug [9]. The effectiveness of oral TMZ treatment is confirmed by its high bioavailability to the CNS (20-40% of plasma exposure) [9] [19]. BCNU is also relatively small and lipophilic[11] and has a molecular weight of 214.049 daltons. It has been hypothesized that the passage of

BCNU through the BBB is allowed primarily due to its small molecular structure and interaction with cell transmembrane proteins.

The therapeutic potential of DOX is hindered greatly by the BBB when the drug is administered systemically. The doxorubicin molecule has a molecular weight of 532.52 daltons, and is much larger than both TMZ and BCNU. Unlike TMZ, DOX is non-lipophilic and has a lower bioavailability. Its non-lipophilic structure and relatively large molecular size restrict DOX from easily crossing the BBB. This results in a need for high systemic doses and increases the incidence of harsh side-effects that occur before the drug is even able to reach therapeutic levels in the brain tissue.

1.4.2 Drug Stability

The chemical stability of chemotherapeutic agents is important from an experimental and clinical point of view. Accurate knowledge of the half-lives of these drugs in biological fluids facilitates the task of formulation during pre-clinical development and enables prediction of clinical efficacy prior to *in vitro* cell studies. Developmental drugs with extremely short half-lives may lack clinical relevance because they degrade long before the drug is able to reach the tumor site. Drug stability can be increased by protecting the chemotherapeutic agent from the surrounding environment. Doxil®, a liposomal formulation of DOX, and Gliadel®, a polymer-BCNU composite, are two novel technologies that work to address the issue of chemical stability. Both formulations will be discussed in the following sections.

1.4.3 Drug Distribution and Payload

Even if chemotherapeutic agents are able to cross the BBB and are stable enough to reach the primary tumor site, malignant gliomas are known to penetrate and invade brain tissue surrounding the main tumor mass. These migratory cells commonly appear 2 to 3 cm away from the parent tumor and are the main cause of progression of primary GBM cells and recurrence after surgical resection [6]. Conventional chemotherapeutic treatment strategies (IV and oral) have been insufficient to achieve

the necessary drug payload needed to target migratory cells. Better techniques are urgently needed.

Localized drug delivery and convection enhanced drug delivery (CED) are two state-of-the-art methods that have been developed to enhance drug exposure time, payload, and distribution. Chemotherapeutic agents are conventionally administered directly to the tumor site by devices implanted near the tumor bed. CED is another form of local delivery that is achieved by infusion of drug solution through an implantable catheter that is attached to an external drug reservoir. Localized drug delivery methods are able to deliver high payloads of drug with long exposure times directly to the tumor bed but suffer from limited drug distribution. CED can theoretically achieve higher drug distribution than local delivery but also suffers from unpredictable fluid partitioning in the brain, tissue damage caused by high infusion pressures (up to 70mmHg) [20], and increased incidence of intracranial infection. A theoretical graph showing the qualitative contrast in drug distribution between these two methods along with the advantages and disadvantages of both is presented in Figure 1-4. The development of drug delivery devices that are capable of exploiting the positive aspects of these two methods is an exciting treatment modality for GBM therapy that will be addressed in this work.

1.5 Novel Chemotherapeutic Delivery Methods

The problems associated with chemotherapeutic treatment of GBM can be addressed by developing new methods of drug delivery. Local intracranial administration of chemotherapy directly to the tumor mass circumvents the BBB and decreases side-effects caused by systemic drug infusion. Innovative techniques for localized drug delivery can also introduce high dose chemotherapy with controllable drug distribution profiles to malignant glioma. Encapsulation of drug using polymeric materials shields the drug from the outside environment and increases drug stability and blood circulation times *in vivo*. Experimental research has produced clinically-relevant, FDA-approved drug formulations and devices that directly address these issues. The

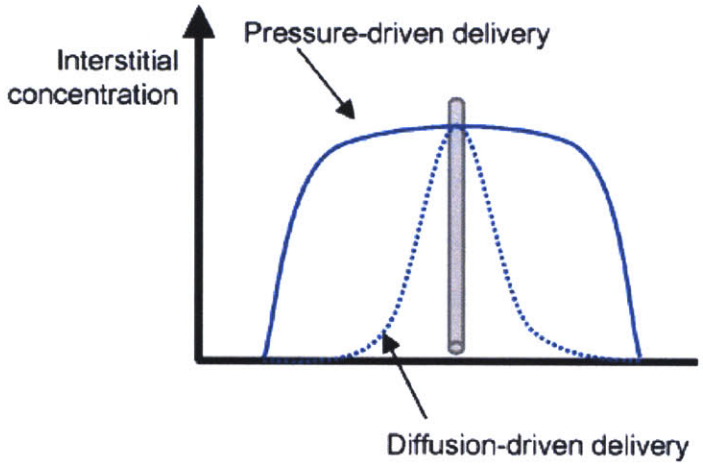

	Advantages	Disadvantages
Polymeric-controlled release	• Sustained drug release • Define release kinetics • Tunable release properties • Low invasiveness • Low peak drug release limits tissue damage • Biocompatible • Localized delivery	• Poor drug penetration • Drug dosage limited by implant size
Convection-enhanced delivery	• Large drug distribution volume • Flexible therapy protocol • Consistent drug concentration	• Invasive • Long infusion times • Potential high intracranial pressures • Unpredictable drug distribution

Figure 1-4: Pressure-driven vs. Diffusion-driven drug delivery concentration profiles [20][21]

devices and formulations important to this thesis will be discussed within the context of the previously selected chemotherapeutic drugs.

1.5.1 Enhancing Carmustine Delivery (Gliadel® Wafer)

One of the most important revolutions in brain cancer therapy has been the development of localized delivery of BCNU directly to the GBM tumor bed. Initial research into the use of drug-impregnated polymer systems as a method to achieve localized drug delivery following surgical resection led to the successful development and FDA approval of the Gliadel® wafer in 1996 [12]. The Gliadel® approach allows for continuous delivery of BCNU from a poly[bis(p-carboxyphenoxy)] propane-sebacic acid] p(CPP:SA) copolymer matrix [22]. Gliadel® devices measure 1.45 cm by 1mm, and the geometry of the brain cavity limits the maximum number of implanted wafers to eight [23]. The devices are implanted around the tumor bed after debulking surgery, and therapy is supplemented with postoperative radiation. The p(CPP:SA) polymer matrix hydrolyzes over time into non-toxic soluble monomers that are then metabolized by the body as BCNU is released from the device.

Gliadel® drug delivery devices address the issues of low drug stability and low drug exposure times to tumor. The half-life of systemically-administered BCNU is 12 minutes, and research has proven that BCNU delivered from the Gliadel® wafer achieved drug concentrations that were log orders higher than the systemic dose, suggesting that the p(CPP:SA) polymer matrix protected BCNU from degradation [22]. BCNU is released over a period of 2-3 weeks when delivered using the Gliadel® wafer, a significantly longer exposure time than that of systemically administered BCNU [22]. The ability of this technology to overcome some of the limitations of conventional chemotherapy along with its proven clinical efficacy made Gliadel® the first new treatment approved for brain tumor therapy in over 20 years [12].

The Gliadel® wafer drug delivery system is not without its share of limitations. The wafers are thin and fragile, and anecdotal evidence notes that surgical implantation of the wafers is extremely difficult to perform without breaking the devices. Broken wafers contribute to increased intracranial edema and a potentially toxic

"burst" release of chemotherapy. The unpredictable drug release rates associated with broken wafers has a detrimental effect on patient QOL and can lead to fatal clinical complications.

The total drug payload offered by Gliadel® is also cause for concern. A single wafer contains only 3.85% BCNU by weight, and assuming that the maximum number of wafers are implanted, the total dosage is near 62 mg of BCNU[24]. A typical surgical debulking session will be unable to remove enough tissue to house eight Gliadel® wafers in the resection site, further reducing the total drug payload. It is interesting to note that during development of Gliadel®, higher doses were found to be efficacious in animal models, but a much lower dose of 3.85% was used in humans without extensive investigation into dose escalation experiments. A 20% BCNU-loaded wafer (the confirmed maximum tolerated dose in humans) with experimentally proven efficacy is now undergoing clinical trials in humans[12], but one has to question why these experiments were not performed before FDA approval of the 3.85% wafer was granted.

1.5.2 Enhancing Doxorubicin Hydrochloride Delivery (Doxil®)

A liposomal IV formulation of doxorubicin was developed in an effort to both decrease the detrimental myocardial toxicity associated with the drug and to increase its blood circulation time. This formulation, Doxil®, consists of doxorubicin hydrochloride encapsulated in a liposome sphere that is composed of hydrogenated soybean phosphatidylcholine, cholesterol, distearoylphosphatidylethanolamine, and a surface-coating of polyethylene glycol (PEG) [25]. Each of the components in this novel drug delivery system carry out specific functions, all of which contribute to the higher efficacy found with Doxil® when compared to free doxorubicin.

The doxorubicin molecule in the Doxil® formulation is no longer used in its free-base form but is formulated with a hydrochloride salt. This formulation greatly increases the solubility of doxorubicin and leads to higher drug loading into the liposome aqueous space. The presence of the liposomal layer shields the encapsulated doxorubicin from the surrounding environment and may increase drug stability. The

final component, the surrounding PEG layer, increases blood circulation time by attracting water molecules that shield the liposomes from detection and destruction by the immune system.

Doxil® has been used as an experimental chemotherapy for convection enhanced drug delivery. U-251MG and U-87MG brain tumor cell lines were implanted intracranially in nude rats prior to Doxil® administration. Results showed that intracranial convection-enhanced delivery of DOX resulted in wider drug distribution than free DOX and decreased tissue damage at the infusion site. Liposomal encapsulation of DOX also allowed for long-term sustained drug release that was not observed in the free DOX group. Statistically significant prolongation of survival was present in both glioma xenograft groups[26].

Chapter 2

Device Concept and Engineering

The main problems associated with systemic chemotherapeutic delivery were discussed in the previous chapter, and include debilitating side-effects, poor patient QOL, non-efficacious drug exposure time, insufficient total drug payload, and only modest increases in patient survival. Oral systemic delivery of TMZ requires large systemic doses and produces unacceptable side-effects without curative outcomes. Localized drug delivery through the use of implantable devices such as Gliadel® offers a number of advantages over systemic drug delivery methods, but also suffers from its own set of drawbacks. Drug distribution and payload delivered by Gliadel® wafers is too low, the devices are extremely large and fragile, and the use of Gliadel® in recurrent GBM patients has not shown a statistically significant benefit in survival between patients receiving Gliadel® versus placebo [27].

CED has been studied as an alternative to local implantation of drug delivery devices. The catheterization necessary for convection enhanced delivery of Doxil® greatly increases the risk of intracranial infection. Issues associated with catheter blockage by tissue and drug partioning in the brain further limit the effectiveness of convection enhanced delivery[20]. A phase III randomized clinical trial found no significant difference in patient survival between Gliadel® and CED of cintredekin besudotox[20].

The device presented in this thesis aims to address the disadvantages of conventional drug delivery by development of an implantable, biodegradable, controlled

release, polymeric microcapsule that delivers either TMZ or DOX following implantation into the brain. It is hypothesized that device implantation around the periphery of the tumor bed may be able to achieve both high local drug concentrations and drug distribution profiles that rival CED. The microcapsules are implanted following surgical tumor resection. Diffusion-controlled release allows for tunable drug delivery kinetics that are manipulated through changes in the number and diameter of orifices in the microcapsule device.

2.1 Diffusion-Controlled Devices

The release of drug from microcapsules by diffusion requires establishment of a concentration gradient between the inside of the device (where drug is stored) and the surrounding environment. According to the second law of thermodynamics, in order to maximize entropy this gradient must induce migration of drug from areas of high drug concentration (inside the microcapsule reservoir) to areas of low drug concentration (the surrounding brain tissue)[28]. This phenomenon can be expressed mathematically through the use of Fick's First Law of Diffusion.

The flux, or rate of change of a solute across a boundary is defined as,

$$J = \frac{d\left(\frac{Q}{A}\right)}{dt} \tag{2.1}$$

where J is the material flux, measured in $\frac{g}{m^2\,s}$. "A" represents the cross-sectional area of diffusion. Q represents the amount of material (drug) that flows through or across A. The amount of material that crosses A over a time interval, Δt is given by,

$$\Delta Q = AJ\Delta t \tag{2.2}$$

Fick's First Law of Diffusion relates the flux of material across a boundary to the concentration gradient, and is defined as,

$$J = -D\frac{\partial c}{\partial x} \tag{2.3}$$

where D is the diffusion coefficient of the drug, measured in $\frac{m^2}{s}$, and $\frac{\partial c}{\partial x}$ is the concentration gradient. Experimental studies approximate the diffusion coefficient, D, of small molecules in solution as $10^{-5}\frac{cm^2}{s}$[28].

Fick's First Law of Diffusion assumes a linear, steady-state change in drug concentration that does not depend on time. We use this approximation in our experiments by assuming that drug in the capsule reservoir is completely saturated, and the fluid surrounding the device is at "infinite sink" conditions at all times. We also assumed uni-directional drug diffusion for simplification. These approximations change the differential expression to the following form,

$$J = -D\frac{\Delta c}{\Delta x} \tag{2.4}$$

where Δc is the concentration of the drug outside the device reservoir less the solubility of drug inside the device, and Δx is the length over which the drug diffuses. Multiplication of the flux, J, by the cross-sectional area for diffusion, A, gives the drug release rate from microcapsule devices, measured in $\frac{g}{s}$. The application of Fick's First Law of Diffusion to tailor the drug release kinetics of our microcapsules through changes in orifice number and diameter will be discussed in the following chapter.

2.2 Chemotherapeutic Drug Selection: Temozolomide and Doxorubicin Hydrochloride

2.2.1 Temozolomide

TMZ is the current state-of-the-art chemotherapetic agent for systemic treatment of GBM, and was the first molecule chosen for release from the microcapsule devices developed in this thesis. The chemical properties, structure, and mechanism of action for this drug were presented in the previous chapter. The oral formulation of TMZ, Temodar®, was initially developed out of the need for more potent chemotherapeutics with better activity against GBM than BCNU. Temodar® is available in six different

doses which range from 5 mg to 250 mg[29]. This oral formulation contains drug excipients and preservatives in addition to TMZ powder. Temodar® exhibits modest side-effects, higher bioavailability, and increased penetration through the BBB when compared with systemically administered BCNU. It has subsequently displaced BCNU as the standard in chemotherapeutic treatment of GBM.

It has been hypothesized that local delivery of TMZ may dramatically increase its effectiveness against GBM, much in the same way that research into localized BCNU therapy lead to FDA-approval of Gliadel®. Our research collaborators at Johns Hopkins University were the first to demonstrate that local delivery of TMZ from polymer-impregnated wafers was efficacious and superior to oral TMZ administration in a rodent model of GBM [30]. The TMZ-polymer composite wafers developed by the Hopkins group use the same polymer matrix as the Gliadel® system and have a maximum drug payload of 5mg TMZ. The small drug payload and non-tunable drug release kinetics of the wafer approach have led to the microcapsules developed in this thesis. *In vitro* and *in vivo* experiments were conducted to compare the efficacy of TMZ delivery from our microcapsule delivery system against oral Temodar® and the Hopkins TMZ-polymer composite wafers.

2.2.2 Dose Escalation

We hypothesized that one of the main reasons for the failure of chemotherapeutic treatment of GBM is due to insufficient drug payload delivery to the tumor site. Systemic-to-localized delivery dose escalation calculations were performed in order to examine the feasibility of delivering the entire oral TMZ treatment regimen from locally-implanted polymer wafers and micro-capsule devices. These calculations are detailed below.

A phase III clinical trial published in the New England Journal of Medicine found the following TMZ dosing schedule to be efficacious in GBM patients: 75mg/m^2/day, given 7 days/week for 7 weeks. After a 4-week break, patients were given 150mg/m^2/day for 5 days every 28 days. The final dosage was 200mg/m^2/day for 5 days every 28 days[15]. This final regimen was repeated up to 5 times. This schedule was used for

the systemic-to-localized delivery dose escalation calculations in this thesis.

In order to calculate the final required human TMZ oral dose, a few assumptions must be made. In this present work, an average weight of 86.6 kg was used for human male dose escalation, and an average weight of 74.4 kg was used for a human female. A body-to-mass index (BMI) of 22 $\frac{kg}{m^2}$ was used for both males and females[31]. The resulting body surface area (BSA) values are given by the following equations,

$$\text{Human Male: } 22\frac{kg}{m^2} \times \frac{1}{86.6kg} = 3.93636\ m^2 \tag{2.5}$$

$$\text{Human Female: } 22\frac{kg}{m^2} \times \frac{1}{74.4kg} = 3.38182\ m^2 \tag{2.6}$$

where BSA values are subsequently used for calculation of the required systemic TMZ doses in males and females.

The total systemic TMZ payload for a human male is given by the equations,

$$\text{a. } 75\frac{mg}{m^2 \times day} \times 3.93636\ m^2 \times 7\ days = 2.07\ \frac{g}{week} \times 7\ weeks = 14.5g \tag{2.7}$$

$$\text{b. } 150\frac{mg}{m^2 \times day} \times 3.93636\ m^2 = 590.545\ \frac{mg}{day} \times 5\ days = 2.95g \tag{2.8}$$

$$\text{c. } 200\frac{mg}{m^2 \times day} \times 3.93636\ m^2 = 787.272\ \frac{mg}{day} \times 25\ days = 19.7g \tag{2.9}$$

where (a.) represents the initial dose of 75mg/m^2/day, given 7 days/week for 7 weeks, (b.) represents the second dose of 150mg/m^2/day for 5 days every 28 days, and (c.) represents the third schedule of 200mg/m^2/day for 5 days every 28 days. Summation of equations (1.3)-(1.5) gives a total male systemic TMZ dose of 37.15g. Similar calculations give a total female systemic TMZ dose of 31.88g.

The total, 8 month systemic TMZ dose offers a starting point for calculating the total dose needed for delivery from locally-implanted devices. Polymer drug delivery wafers and microcapsules provide localized delivery of TMZ that bypasses systemic metabolism and the BBB. The bioavailability and BBB-partitioning of TMZ are assumed to be nearly 100% and 35%, respectively[32][33]. A 100% bioavailability suggests that the entire oral drug payload reaches the systemic circulation, and a

35% BBB-partitioning value assumes that 35% of the circulating drug reaches the cerebrospinal fluid (CSF). Pharmacokinetic models and experiments have confirmed these values. Usage of the assumed systemic bioavailability and BBB-partitioning values allows calculation of the total required local TMZ dose by the equations,

$$\text{Human Male: } 37.15g \times 0.35 = 13g \tag{2.10}$$

$$\text{Human Female: } 31.88g \times 0.35 = 11.16g \tag{2.11}$$

where a total of 13g TMZ for males and 11.16g TMZ for females needs to be delivered locally from polymer wafers and microcapsules.

The polymer wafers developed at Johns Hopkins University can deliver a maximum TMZ payload of 5mg, and the microcapsule system can deliver up to 12mg of TMZ. 2600 wafers or 1084 micro-capsules would need to be implanted in order to achieve the required 13g payload in a human male brain. Implantation of this number of devices is not surgically feasible, but despite this shortcoming, local delivery of TMZ offers an important starting point for improving drug delivery to GBM by demonstrating that local delivery extends the survival of tumor-challenged animals more so than conventional oral delivery. It may also not be necessary to deliver the entire, 8 month course of chemotherapy locally, and the microcapsule system could be used as an adjuvant therapy along with oral TMZ and radiation. This would substantially reduce the number of implanted devices. The need for more potent chemotherapeutic molecules with substantially lowered doses, such as doxorubicin hydrochloride, led to the selection of DOX as the second model chemotherapeutic for delivery from microcapsule devices.

2.2.3 Doxorubicin Hydrochloride

Recent clinical studies of intratumoral infusion of 5mg DOX over ten days were shown to increase patients' time to disease progression by 36±2 weeks, and the median survival of all ten patients enrolled in the study was 36.2±22.4 weeks [34]. Localized

delivery of DOX also resulted in no significant adverse side-effects[34]. This method offers a way to decrease the development of cardiac toxicity caused by systemic DOX infusion. The DOX dosage used in this study is substantially lower than the currently prescribed TMZ dose.

The microcapsules fabricated in this thesis can theoretically be loaded with a much larger payload (20 mg) than used in the Voulgaris study and can also be tuned to release this payload directly to the tumor site over a chosen amount of time. Delivery of DOX from microcapsule devices may allow for administration of the entire drug therapy from one device instead of the thousands needed for satisfactory TMZ delivery. The extremely low BBB-partitioning of DOX along with its high systemic toxicity and low local dosage requirements make it an attractive molecule for localized drug delivery from our microcapsules.

2.3 Material Selection: Poly-L-Lactic Acid and Liquid Crystal Polymer

Development of any implantable device requires careful selection of suitable materials for its construction. The material should meet the following criteria: 1) Must be biocompatible. 2) Must provide a hermetic barrier that prevents unpredictable drug leakage. 3) Must protect the drug from degradation by the surrounding environment. 4) Must maintain mechanical and structural integrity throughout the entire course of drug therapy. 5) Must degrade into non-toxic, biocompatible monomers after completion of drug delivery, if the material is biodegradable. 6) Must allow for easy manufacture with precise dimensional tolerances through the use of standard industrial techniques (injection molding, extrusion, etc). The two materials chosen for fabrication of the micro-capsules in this thesis were liquid crystal polymer (LCP), and poly-L-lactic acid (PLLA).

2.3.1 Poly-L-Lactic Acid

Poly(esters) are the best characterized and most widely studied biodegradable polymer system[35]. Poly(lactic acid) (PLA) belongs to this class of polymers, and was one of the first polyesters used for biomedical applications when a patent for its use as a resorbable suture was filed in 1967. Other popular biocompatible polyesters include poly(lactic-co-glycolic) (PLGA) and PLLA. Polyesters have also been extensively used in drug delivery applications. A polymeric drug delivery device developed by Grayson et al, produced resorbable millimeter size devices made of compression-molded PLLA reservoirs with thin PLGA membranes. These devices showed non-toxic *in vivo* degradation, and efficacious delivery of BCNU to a rodent glioma model[11] [36].

Lactide monomers are formed by dimerization of lactic acid molecules. These lactide monomers are then synthesized into PLLA through ring-opening polymerization. The polymerization mechanism is shown in Figure 2-1. Ring-opening polymerization

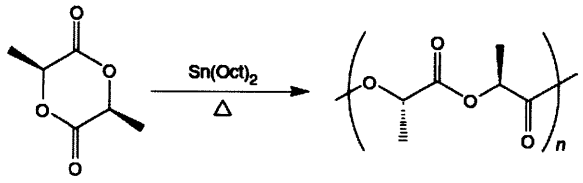

Figure 2-1: Ring-opening polymerization of lactide.
[37]

of the cyclic lactide monomer is usually too slow to produce high molecular weight polymer. The rate of polymerization is commonly increased by adding a catalyst such as stannous octoate to the monomer mixture[35]. Stannous octoate is a biocompatible, FDA-approved food stabilizer that has proven safe for use as a polymerization catalyst. Tin(II) 2-ethylhexanoate has also been used as a catalyst in PLLA polymerization[37].

Naturally occurring lactic acid contains an asymmetic α-carbon that is described as the D or L form, in stereochemical terms. PLA contains a mixture of L and D forms, while PLLA is a homopolymer of the L form. The difference in stereochemistry between PLA and PLLA has direct effects on the physical properties of the two polymers. For example, the melting temperature of crystalline PLLA is 170 °C and

PLA is completely amorphous, with no observable melting point[35].

PLLA is considered more biocompatible than PLA and PDLA because the L-form is naturally occurring. The PLLA polymer is derived from monomers that are natural metabolites of the body. After degradation of PLLA, the resulting hydroxy acid monomers are readily absorbed by the body. The degradation of PLLA occurs primarily through bulk degradation with hydrolytic scission of the polymer backbone[35]. The degradation rates of the PLLA used in our microcapsule devices depend on device geometry and thickness, injection molding process conditions, and the resulting crystallinity of the polymer. The PLLA purchased from Lakeshore Biomaterials that is used in this work has a degradation timeframe of greater than 24 months. The microcapsule devices are engineered to release the entire drug payload after a maximum of two weeks, meaning that the polymer housing will fully degrade months after drug therapy is complete.

2.3.2 Liquid Crystal Polymer

Previous experimental studies in our laboratory found that PLLA drug delivery devices loaded with carmustine failed to pervent partitioning of drug through the polymer housing. This led to unsatisfactory drug release profiles and unacceptable drug leakage. The hermeticity of these devices was compromised, which resulted in the need to re-evaluate the material choices for use in the current microcapsule delivery devices.

Liquid crystal polymers (LCP) are a unique class of polymers that exhibit liquid crystal phase characteristics either in solution or in the melt. A substance's liquid crystalline state is defined by the one- or two-dimensional long-range molecular order that is maintained above the material's crystalline melting point[38]. Liquid crystalline behavior in polymer systems is due mainly to molecular rigidity of the polymer chains that excludes more than one molecule from occupying a certain volume. Molecular shape anisotropy is the main requirement for a polymer to show liquid crystalline behavior.

The molecular arrangement of polymer chains in the liquid crystalline phase is

directly related to the polymer's physical behavior and properties. Liquid crystal polymer melts have lower viscosities than melts of random-coil polymers because the liquid crystal polymer chains are able to align with the direction of flow. Industrial processing of low-viscosity liquid crystal materials is much easier than with random-coil polymers. The extension and orientation of polymer chains during processing also yields highly crystalline solid polymers with extremely high modulus and strength values.

The barrier properties of LCP make it an attractive alternative material to PLLA for use in the fabrication of drug delivery devices. LCP polymers exhibit very low moisture absorption (0.02%) and have low moisture permeability[39]. LCP also has excellent chemical resistance to most acids, bases, and solvents[39], and has been used in moisture-resistant medical packaging products[40]. The strong barrier properties and great chemical resistance of LCP suggest that micro-capsules fabricated from this material may be able to successfully store the drugs used in this current work. Experimental drug leak tests were performed in order to test the reliability and hermeticity of LCP polymer microcapsules.

Unlike PLLA, LCP polymers are not biodegradable. Despite this, the LCP used for the devices presented in this thesis (Vectra MT1300) is bioinert, and has passed the USP (United States Pharmacopeia) class VI biocompatibility test. This test consists of intracutaneous injection, systemic LCP injection, and implantation tests. The *in vivo* compatibility of LCP with rodent brain tissue was qualitatively assessed in this thesis by checking for the presence of fibrous tissue growth around the microcapsule and measuring animal survival times when implanted with unloaded microcapsules. The results of these experiments are presented in the results chapter.

2.4 Tumor Model Selection: 9L Gliosarcoma

The selection of a clinically-relevant rodent tumor model is crucial to testing the efficacy of drug delivery devices. There is no currently available animal tumor model that is able to exactly simulate human GBM. A wealth of information has been

obtained from experimental animal GBM models. The use of animal models has led to the development of new therapies and treatment strategies for human GBM. A general consensus among researchers and clinicians states that valid GBM animal models should be derived from glial cells, display glioma-like growth characteristics within the brain, possess predictable and reproducible tumor growth rates, and their response to therapy should closely simulate that of human brain tumors[41].

The 9L gliosarcoma xenograft model used in this work is one of the most widely used of all rat brain tumor models. It can be grown both *in vitro* and *in vivo* which makes it useful for a wide variety of studies ranging from *in vitro* drug resistance experiments to *in vivo* intracranial pharmacokinetic studies[41]. The 9L gliosarcoma is an attractive experimental model because it grows rapidly and unaltered Fischer rats can be used for *in vivo* studies. This allows for quick experimental studies and the use of inexpensive rodents.

The main problem associated with the use of the 9L xenograft cell line is its non-invasive *in vivo* growth pattern[41]. Human glioma cell lines such as U87 and SF-539 are able to invade the surrounding ECM; this growth is also commonly observed in GBM patients. The use of human glioma in rodents requires the use of immunocompromised, "nude" animals that are more expensive than Fischer rats and are also more prone to opportunistic infections. U87 gliomas grow slower than 9L gliosarcomas *in vivo* which results in much longer drug efficacy trials when survival is the primary metric. The 9L model was chosen for use in this thesis as a relatively quick target to assess efficacy of our drug delivery devices, and the U87 model will be used in future long-term survival experiments.

Chapter 3

Microcapsule Design and Manufacture

Two types of drug delivery microcapsules for treating GBM were developed in this work. One device is fabricated from liquid crystal polymer (LCP), and the other from a biodegradable polymer, poly(l-lactic) acid (PLLA). The design of both devices includes a drug-storage reservoir and a cap used to seal the device from the outside environment. Drug is released through circular orifices that are either molded or laser drilled into each device. The rate of drug delivery is controlled by the diameter of the orifice, the number of orifices, and the drug formulation. The inner volume of the reservoir measures 15 μL, which allows for higher drug loading per device volume when compared to previous polymer drug delivery devices[36][30]. The higher drug loading capability facilitates the local delivery of large drug payloads to tumors, which is critical for effective chemotherapeutic treatments. These devices are engineered using Fick's First Law of Diffusion to achieve desired release kinetics that fit the need of disease treatment.

3.1 Design

3.1.1 Temozolomide-Releasing Devices

The SolidWorks 3D CAD software package was used to design the microcapsule devices. The first-generation microcapsule devices designed to release TMZ allowed for uni-directional drug delivery from a single 889 μm diameter orifice in the device cap (Figure 3-1a).

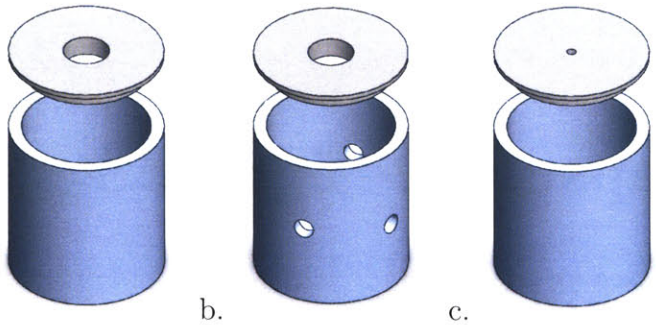

Figure 3-1: Microcapsule device design. a) First Generation TMZ Device. b) Second Generation TMZ Device. c) DOX Device

Results from the first TMZ *in vivo* efficacy study led to the hypothesis that multi-directional drug delivery would increase the effectiveness of the microcapsules against the 9L gliosarcoma model. This led to the fabrication of second-generation TMZ-releasing microcapsules with a single 889 μm diameter orifice cap and four 403 μm diameter orifices around the circumference of the microcapsule reservoir (Figure 3-1b).

3.1.2 Doxorubicin Hydrochloride-Releasing Devices

Microcapsule devices for delivery of DOX were also designed using the SolidWorks software package. DOX has a higher aqueous solubility than TMZ, which led to the use of smaller orifice diameters in the DOX-releasing devices. The microcapsules used for delivery of DOX have a single 180 μm diameter orifice in the device cap (Figure 3-1c). This smaller orifice allows for long-term controlled drug delivery over a period of 2 weeks without a "burst" release of drug.

3.1.3 Microcapsule Device Fabrication

Metal mold cavities were fabricated based on the previously mentioned SolidWorks designs. PLLA and LCP molten polymers were injection molded into their final microcapsule form at microPEP (East Providence, RI). The injection molding process allows for high precision device production, giving reliable and consistent results, including very small tolerances in payload volume and orifice diameter. The device dimensions are shown in Table 3.1. The millimeter-scale dimensions were chosen to allow for intracranial device implantation in Fischer 344 rats.

	Reservoir	Cap
Inner Diameter (mm)	2.49	2.5
Outer Diameter (mm)	3	2.97
Sidewall Thickness (mm)	0.245	n/a
Height (mm)	2.86	n/a
Inner (full) Thickness (mm)	n/a	0.3
Outer (lip) Thickness (mm)	n/a	0.09

Table 3.1: Microcapsule device dimensions

Injection molding is also capable of fabricating large numbers of devices in single process runs. 180 μm diameter orifice devices were fabricated directly in the mold cavity, while a drill press equipped with a #65 (0.0350 decimal equivalents) drill bit was used to manufacture the 889 μm diameter orifice devices. An excimer laser system (TeoSys Engineering LLC) operating at 193nm was used in order to manufacture the four 403 μm diameter orifices around the circumference of the microcapsule reservoirs.

3.1.4 Drug Loading

A metal hopper was designed for use in loading chemotherapeutic drug into the microcapsule reservoirs. An empty device reservoir was placed into the hopper mold cavity, then a metal funnel was placed on top of the cavity. Precise amounts of solid drug (12mg of TMZ or 1mg of DOX for *in vivo* experiments) were dispensed into the funnel, and a tamping metal tool was used to compress the drug inside of the microcapsule reservoir. Excess drug was cleared from the device reservoir by sliding

the funnel across the device and shearing the remaining drug.

3.2 Tailoring Drug Release Kinetics

The appropriate dimensions of the microcapsule orifice(s) and drug formulation depend on the drug and treatment characteristics. The drug delivery devices developed in this work were precisely tailored to function within the properties of the drug and needs of the disease. Several pieces of information; drug solubility, drug stability and the desired release rate, were critical to determining the final design of the devices. Drug solubility and stability experiments will be presented in detail in the following section. Fick's First Law of Diffusion was used to calculate the theoretical release rate of drug from microcapsule devices.

3.2.1 Temozolomide-Releasing Microcapsules

Single-Hole Devices

The TMZ-impregnanted polymer wafers developed by Brem et al. were chosen for comparison with our first generation microcapsule devices. An average release rate of 1.17 mg per day from these wafers was shown to prolong rodent survival, and this drug flux was used as a model delivery rate from the microcapsules. The theoretical release rate of TMZ from single, 889 μm diameter orifice microcapsules was calculated by using Fick's First Law of Diffusion,

$$J = -D\frac{\Delta c}{\Delta x} \tag{3.1}$$

$$\Delta c = -8.82\frac{mg}{ml} \tag{3.2}$$

$$\Delta x = 0.04cm \tag{3.3}$$

$$D = 10^{-5}\frac{cm^2}{s} \tag{3.4}$$

where Δc is equal to -8.82 $\frac{mg}{ml}$ for TMZ, Δx is equal to 0.04 cm (the thickness of

the device cap), and D equals $10^{-5}\frac{cm^2}{s}$. Multiplication of these terms gives the flux, J, as $2.205 \times 10^{-3}\frac{mg}{cm^2 \cdot s}$.

The area of diffusion, A, is equal to the area of a circle,

$$A = \pi r^2 \tag{3.5}$$

where, in the case of an 889 μm diameter orifice, A is equal to $6.207 \times 10^{-3} cm^2$.

The release rate of TMZ can finally be calculated by multiplication of the flux, J, by the area of diffusion, A,

$$\text{Release Rate} = J \times A \tag{3.6}$$

and the theoretical release rate of TMZ delivered from an 889 μm diameter orifice device is $1.4 \times 10^{-5}\frac{mg}{s}$, or $1.2096\frac{mg}{day}$. This theoretical release rate was used for comparison with the experimentally determined TMZ release rates from the microcapsules.

Multiple-Hole Devices

Multiple orifice microcapsules were fabricated in order to increase the release rate of TMZ. Four additional orifices were laser-drilled around the circumference of the microcapsules to achieve multi-directional drug release. These second-generation microcapsule devices were manufactured with a total of five orifices for drug release: One, 889 μm diameter orifice in the cap and four 403 μm diameter orifices around the circumference of the microcapsule reservoir. The release rate of TMZ from these devices was calculated using the same assumptions and approximations as in the single-orifice case, and was found to be $2.5 \times 10^{-5}\frac{mg}{s}$, or $2.16\frac{mg}{day}$. The multiple-orifice release rate is nearly twice as fast as the single-orifice release rate, and these devices showed statistically significant increases in survival in an *in vivo* rodent 9L gliosarcoma model.

3.2.2 Doxorubicin-Releasing Microcapsules

The literature values of DOX solubility ranged from 50 $\frac{mg}{ml}$ to over 100 $\frac{mg}{ml}$, and the amount of drug needed for experimental determination of solubility was financially unjustifiable. DOX release rates were instead determined using the previously manufactured microcapsule devices. Initial *in vitro* drug release studies showed that DOX release from a single 889 μm diameter orifice device resulted in an unsatisfactory "burst" release of drug over one hour. This type of release is extremely dangerous because the large release of a potent drug over a short time period can cause local tissue necrosis and debilitating side effects. A single 180 μm diameter orifice microcapsule was used for delivery of DOX, and was tested *in vitro* and *in vivo*.

Chapter 4

Materials and Methods

4.1 Materials

Temozolomide (TMZ) was provided by the National Cancer Institute (NCI, Bethesda, MD). HPLC-grade water, ammonium acetate, acetonitrile, hydrochlorothiazide, and doxorubicin hydrochloride (DOX) were purchased from Sigma-Aldrich. Phosphate buffered saline (PBS), fetal bovine serum (FBS), and pH buffers were purchased from VWR International.

4.2 Device Fabrication

Liquid crystal polymer, LCP, (Vectra MT1300) was purchased from microPEP (East Providence, RI). Poly(l-lactic) acid, PLLA, (100 L) was purchased from Lakeshore Biomaterials (Birmingham, AL). PLLA and LCP polymer microcapsule devices were injection molded into their final form at microPEP (East Providence, RI).

4.3 Temozolomide Characterization

4.3.1 High Pressure Liquid Chromatography

Two methods were used to quantify TMZ using high pressure liquid chromatography (HPLC). The first method was employed for samples of TMZ in HPLC-grade water, PBS, and pH buffers. 20 μL of sample was quantified at 37 °C on an Agilent 1200 Series HPLC using a Synchropak SCD-100, 5 μm, 150x4.6 mm column (Synchrom, Lafayette, IN, USA), a flow-rate of 0.4 ml/min, 0.01 M ammonium acetate (aqueous):acetonitrile (92:8) mobile phase, and UV absorption at 316 nm. The results from this method were used to construct a standard curve for use in quantification of *in vitro* TMZ release from polymer microcapsule devices.

A second method was used for quantification of TMZ in FBS. The same chromatographic conditions were used with the addition of sample clean-up and preparation steps. 200 μL of TMZ sample was added to 100 μL of 100μg/mL hydrochlorothiazide. The resulting solution was vortexed and then spun at 4500 G using a MiniSpin centrifuge (Eppendorf) at room temperature for 1 minute. Samples of the supernatant were analyzed on the HPLC (these methods were adapted from Kim et al) [42].

4.3.2 Temozolomide Stability

Drug stability studies were conducted in HPLC-grade water, PBS, and FBS. Approximately 1 mg of TMZ was added to 2 mL of solvent. The resulting solutions were stored at 37 °C and sampled periodically over a 14 hour time period. Samples were analyzed for TMZ content by the HPLC methods described above. Quantification of the internal standard hydochlorothiazide demonstrated that no appreciable losses occurred due to FBS sample preparation.

4.3.3 Temozolomide Solubility

Saturated solutions of TMZ were prepared in pH 1, 2, 3, 4, and 5 buffers and in pH 7 HPLC/MS grade water. Each buffer was analyzed using the HPLC method

described above to determine the presence of any interfering peaks. No interfering peaks were found. Approximately 10 mg of TMZ were added to 500 μL of each buffer solution at 37 °C. Each solution was left for 20 minutes at 37 °C with intermittent vortexing. Solutions were then spun at 10,000rpm for 5 minutes using a MiniSpin centrifuge. Drug precipitate was present in all samples. Samples for HPLC analysis were prepared from the supernatant at the following dilutions; pure supernatant, 1:5, 1:10, and 1:20. All dilutions were made with the appropriate buffer pre-heated to 37 °C. Samples that read in the linear range of the standard curve were used to calculate solubility by adjusting the read concentration by the appropriate dilution factor.

4.4 Doxorubicin Hydrochloride Characterization

4.4.1 Fluorescence Assay

The concentration of doxorubicin in HPLC-grade water was analyzed by fluorescence assay. Measurements were made on a Synergy 4 fluorescence plate reader (BioTek Instruments, Inc.) with a programmed internal temperature of 37 °C. Intensity of fluorescence emission was determined at 590nm with an excitation wavelength of 470nm [43]. Fluorimetric intensity readings were converted to mg/ml concentrations by interpolation with the readings of a standard curve of doxorubicin in the linear range.

4.5 *In Vitro* Drug Release Kinetics

4.5.1 Temozolomide-Polymer Composite Wafers

TMZ was incorporated into a polyanhydride CPP:SA polymer at a concentration of 50% (w/w) by methods described previously [44]. The polymers were then pressed into a disc shape weighing approximately 10 mg. Total drug payload was approximately 5mg per wafer. Wafers were placed into 2ml of HPLC/MS-grade water to

begin release studies. The sample bath was removed and refilled periodically for analysis of the drug concentration present in each sample. Samples were stored in liquid nitrogen until analysis. Interpolation of the readings with a standard curve of TMZ was used to quantify the amount of TMZ released over multiple days.

4.5.2 Temozolomide-loaded Drug Delivery Devices

Temozolomide was loaded into LCP single- and multiple-hole polymer microcapsules for *in vitro* drug release characterization. Drug payload in each device was 12mg. Single-hole devices had an orifice diameter of 889μm in the device cap. Multiple-hole devices had a single 889μm-diameter cap orifice and four 403μm-diameter orifices around the circumference of the device reservoir. After temozolomide was loaded into each device, and caps were sealed to the reservoir with UV-curable epoxy (1-20542 UV Curing Cationic Epoxy, Dymax Corp, Torrington, CT). Devices were exposed to UV light for a cure time of 90 seconds. Control devices with epoxy-sealed orifices were fabricated for leak tests to examine the hermeticity of the UV epoxy and polymer reservoir. A vacuum pump was used to remove residual air from the devices. Devices were placed into 2ml of HPLC/MS-grade water to begin release studies. The sample bath was removed and refilled periodically for analysis of the drug concentration present in each sample. Samples were stored in liquid nitrogen until analysis. Interpolation of the readings with a standard curve of TMZ was used to quantify the amount of TMZ released over multiple days.

4.5.3 Doxorubicin Hydrochloride-loaded Drug Delivery Devices

DOX was loaded into LCP single-hole drug delivery devices with a single 180μm diameter orifice for *in vitro* characterization of release kinetics. Drug payload in each device was 1mg. After DOX was loaded into each device, and device caps were sealed to the reservoir with UV-curable epoxy (1-20542 UV Curing Cationic Epoxy, Dymax Corp, Torrington, CT). Devices were exposed to UV light for a cure time of

90 seconds. Control devices with epoxy-sealed orifices were fabricated for leak tests to examine the hermeticity of the UV epoxy and polymer reservoir. A vacuum pump was used to remove residual air from the devices. Devices were placed into 2ml of HPLC/MS-grade water to begin release studies. The sample bath was removed and refilled periodically for analysis of the drug concentration present in each sample. Samples were stored in liquid nitrogen until analysis. Fluorescence spectroscopy was used to quantify the amount of DOX released over multiple days.

4.6 *In Vitro* 9L Gliosarcoma Cell Culture

MTT assay was used to quantify the effect of varying concentrations of DOX on survival of 9L glioma cells cultured *in vitro*. Glioma cells were plated at a density of 3500 cells/well, and DOX diluted in DMEM cell culture media with 10% glucose (Invitrogen) was added to each well 24 hours after initial cell plating. DOX concentrations were: 50μg/ml, 10μg/ml, 5μg/ml, 1μg/ml, 0.5μg/ml, 0.1μg/ml, 0.05μg/ml, 0.01μg/ml, 0.005μg/ml, and control samples with blank growth media. Cells were counted 48 hours following DOX administration in order to quantify the extent of DOX-mediated cell death.

4.7 *In Vivo* Rodent Experiments

4.7.1 Tumor and Device Implantation

9L glioma cells were implanted in the flank of Fischer 344 (Harlan Sprague Dawley, Indianapolis, IN) rats and allowed to proliferate for several weeks until a tumor of approximately 2 cm diameter was grown. The tumor was harvested after euthanasia of the rat and cut into pieces approximately 1 mm^3 in volume. Female or male Fischer 344 rats weighing 150-300 g were anesthesized with intraperitoneal injections of a xylazine/ketamine stock solution, at a concentration of 3-5 ml/kg. The anesthesia stock solution contained 25 mg/ml ketamine hydrochloride, 2.5 mg/ml xylazine, and 14.25% ethanol in 0.9% saline. The heads of anesthesized rats were shaved and

the skin prepped using a betadine scrub. A mid-line incision of 2-3 cm length was made, followed by removal of the underlying membrane layer to leave a clear path for drilling. A 3.5 mm diameter hole was drilled using a motorized power tip and attached stainless steel drill bit. The hole was drilled 2-3 mm lateral to the midline suture and 5 mm posterior from the coronal suture, or 1 mm anterior to the interaural line. A microscope was used to assist in implanting the tumor and drug delivery microcapsule, cap side down, into the intracranial space. Excess CSF fluid and white matter were lightly suctioned to make space for the tumor and device. The skin of the head was closed using autoclips once the implantation was completed, and animals were returned to their cages.

4.7.2 Efficacy of Locally Delivered Temozolomide

Two experiments were conducted in order to determine the effectiveness of locally delivered temozolomide in intracranial tumor-bearing Fischer 344 rodents. The first pilot experiment included nine experimental groups: 1) Control animals with tumor. 2) Animals given oral temozolomide by gavage at a dose of 50mg/kg on days 5-9 after tumor implantation. 3) Animals given two 50%wt TMZ-polymer wafers. 4) and 5) Control animals with tumor and blank LCP/PLLA microcapsules (no drug payload). 6) and 7) Animals given TMZ-filled LCP/PLLA microcapsules on the day of tumor implantation (Day 0). 8) and 9) Animals given TMZ-filled LCP/PLLA microcapsules five days after tumor implantation (Day 5). All microcapsule devices used in this experiment had a total TMZ payload of 12mg and single 889μm-diameter orifice caps. The total number of animals used was 68. Overall animal survival was compared to that of the device-free control group.

The results of the first *in vivo* efficacy experiment were used to design a second *in vivo* experiment with modified drug delivery devices. This second study included four experimental groups: 1) Control animals with tumor. 2) Control animals with tumor and blank LCP microcapsules (no drug payload). 3) Animals given oral TMZ by gavage at a dose of 50mg/kg on days 5-9 after tumor implantation. 4) Animals given TMZ-filled LCP microcapsules on the day of tumor implantation (Day 0). All

drug delivery microcapsules used in this experiment had a total TMZ payload of 12 mg, single 889μm-diameter orifice caps, and four 403μm-diameter drug release orifices around the reservoir of the device. The total number of animals used was 30. Overall animal survival was compared to that of the control group.

4.7.3 Doxorubicin Hydrochloride Toxicity

DOX-loaded, single 889μm-diameter orifice microcapsules were fabricated for *in vivo* drug toxicity studies. A drug payload of 1mg was loaded into each device. Three Fischer 344 rats were used in this experiment. Animals were monitored for neurological and behavioral changes throughout the study, including weight loss, failure to thrive, and wound healing problems. Death was the primary endpoint of the experiment.

4.7.4 Animal Care

All animals were housed in standard facilities and given free access to food and water. Rats were treated in accordance with the policies and guidelines of the Johns Hopkins University Animal care and Use Committee. Each study was terminated at Day 120, and the surviving rats were deemed long-term survivors (LTS). All excised brains were stored in formalin following death prior to histological studies.

4.7.5 Statistical Analysis

Death was the primary endpoint for all *in vivo* efficacy studies. The method of Kaplan and Meier was used to determine the distribution of intervals until death. Statistical analysis (unpaired t-test) was performed using the Prism GraphPad software package.

4.8 Immunohistochemical Analysis

4.8.1 TUNEL Stain

Terminal deoxynucleotidyl transferase dUTP nick end labeling (TUNEL staining) was performed on rat brain tissue samples in order to quantify the ability of TMZ to damage 9L glioma nuclear DNA. The protocol was specifically used for detection and quantification of apoptosis at the cellular level. The TUNEL method works by labeling DNA strand breaks that are caused by exposure to cytotoxic agents such as TMZ. These single or double stranded breaks are identified by labeling the free 3'-OH terminal with modified nucleotides[45]. Counting of cellular nuclei with TUNEL-positive stains allows for quantitative determination of apoptosis. The rat brain tissue used in this study was paraffin-embedded and sliced through the coronal plane before TUNEL analysis. The multi-step staining protocol developed by Heatwole et al was used [46].

Chapter 5

Results

5.1 Temozolomide Physical Chemistry

5.1.1 High Pressure Liquid Chromatography

A typical HPLC chromatograph of TMZ in water is shown. The retention time of TMZ on the Synchropak SCD-100 column was 9.5 minutes when a flow rate of 0.4 ml/min was used. No interfering peaks were present throughout the HPLC analysis.

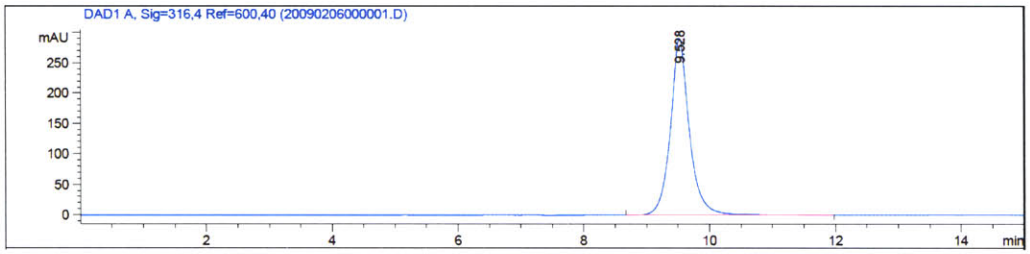

Figure 5-1: TMZ HPLC Chromatograph

5.1.2 Temozolomide Stability

The chemical stability of TMZ was studied in water, PBS, and FBS. The data is presented as normalized area-under-the-curve (AUC) values versus time, and was collected over a period of fourteen hours. Exponential curve-fitting of the water, PBS, and FBS data allowed for calculation of the half-life of TMZ in each of these

solvents. The results show that TMZ was most stable in water, with a half-life of 99 hours, followed by PBS and FBS, with half-lives of 5 and 0.7 hours, respectively. The *in vivo* stability of TMZ calculated by Zhou et al is 0.9 hours[47], which is in close agreement with our calculated value of 0.7 hours for TMZ in FBS.

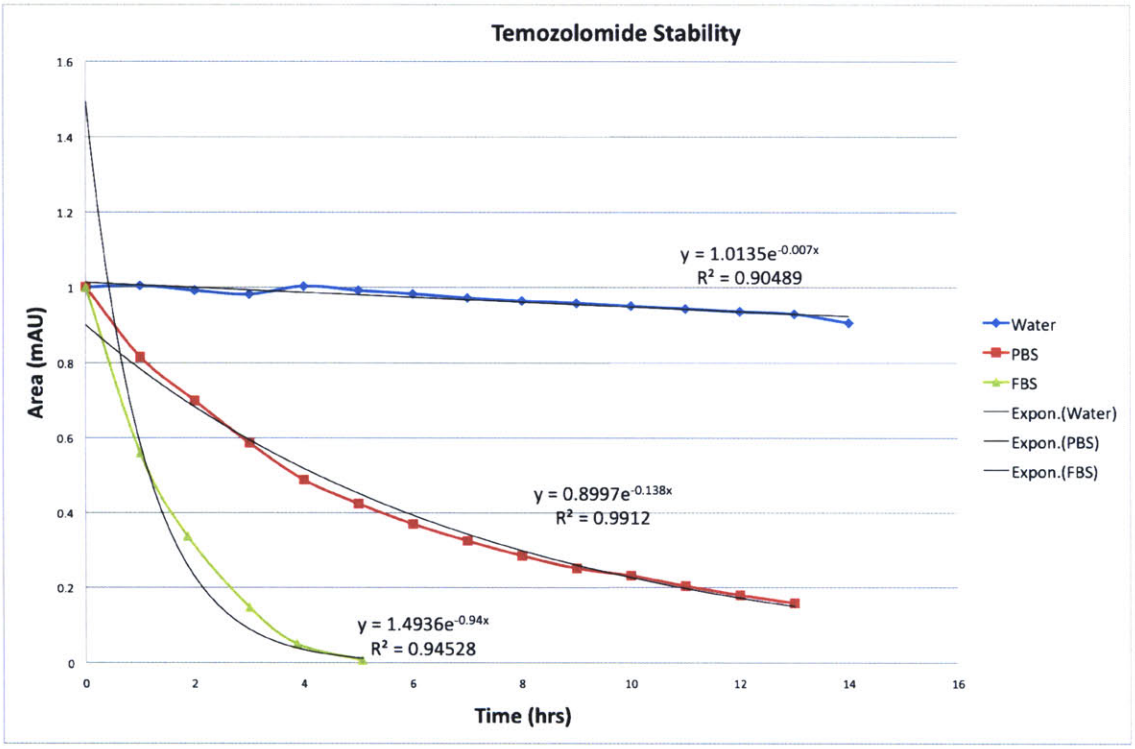

Figure 5-2: TMZ Stability

5.1.3 Temozolomide Solubility

Temozolomide solubility was assessed in pH 1, 2, 3, 4, and 5 buffer solutions and in pH 7 water. Solubility values were calculated by comparing the AUC values obtained using the HPLC system with values from a calibration curve of TMZ in the linear range. These AUC values were then multiplied by the appropriate dilation factor used in each study to produce the final solubility value. The resulting solubility values showed a solubility range of 6.38 mg/ml for TMZ in pH 1 buffer to 11.5 mg/ml for TMZ in pH 3 buffer. The solubility of TMZ in water was 8.82 mg/ml. A solubility of 8.82 mg/ml was used in calculating the theoretical release kinetics for our drug

delivery devices because this solubility corresponds to the expected physiologic pH of 7.

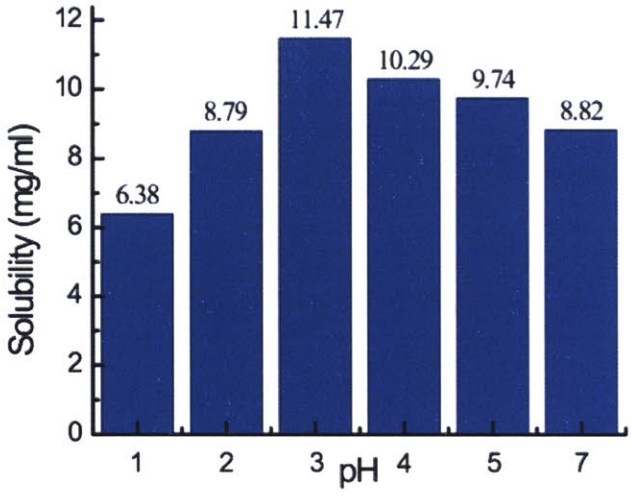

Figure 5-3: TMZ Solubility

5.2 *In Vitro* Temozolomide Drug Release Kinetics

5.2.1 Polymer Wafers

The TMZ-impregnated polymer wafer device developed at Johns Hopkins University served as a metric for comparison with our drug delivery microcapsules. The wafers used *in vitro* and *in vivo* in this thesis had a total payload of 5mg TMZ per wafer. The *in vitro* release of TMZ from these wafers into HPLC-grade water was assayed by HPLC. The number of devices for each group in this experiment was three. Results were reported as average values with standard deviations for each time point. Results showed that 75% of the total drug payload was released after 62 hours. This corresponds to a TMZ mass of 3.75mg.

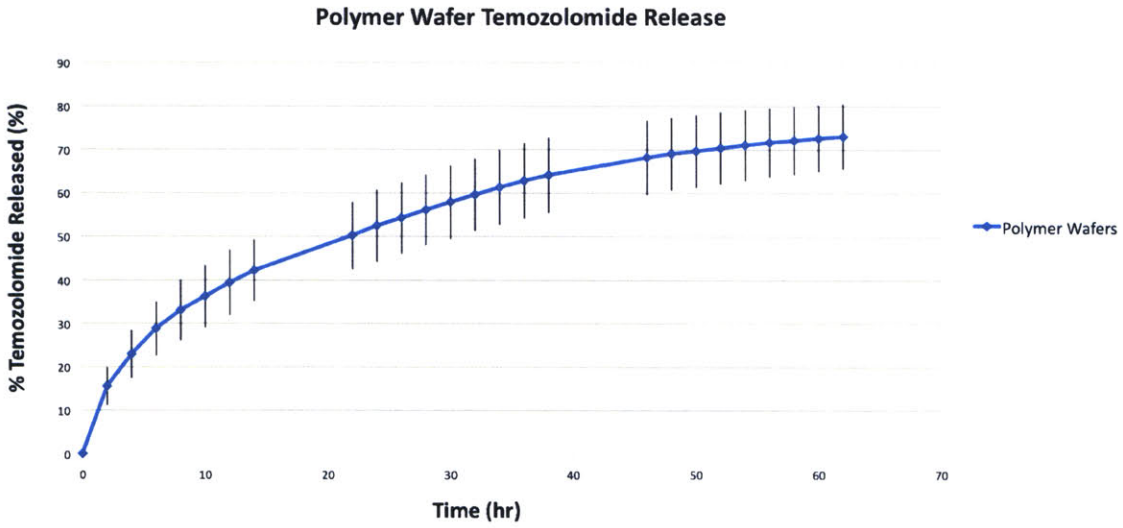

Figure 5-4: Polymer wafer TMZ release into water

5.2.2 Single-Hole Devices

The *in vitro* release of TMZ from single 889 μm diameter orifice LCP drug delivery microcapsules into HPLC-grade water was assayed by HPLC. Control devices with completely sealed orifices were also fabricated in order to test the hermeticity of the UV-curable epoxy. A theoretical release curve based on Fick's First Law of Diffusion was constructed for comparison with experimental drug release data. The mass flow rate calculated from Fick's 1st Law was 50.4 ug/hr. The number of devices for each group in this experiment was three. Results were reported as average values with standard deviations for each time point. The experimental release curves were in close agreement with the theoretical release curve, especially at times before 80 hours. The experimental TMZ release rate during the first 100 hours of release was 36 ug/hr. At this time, 40% of the total 12mg was released. The release rate decreased after 100 hours, with a final drug release of 50% after 175 hours. The devices fabricated for drug leak tests demonstrated that the UV-curable epoxy is capable of sealing the devices and preventing leakage of drug from the devices. No drug partitioning through the polymer housing was detected, suggesting that LCP is capable of storing the drug throughout the length of therapy.

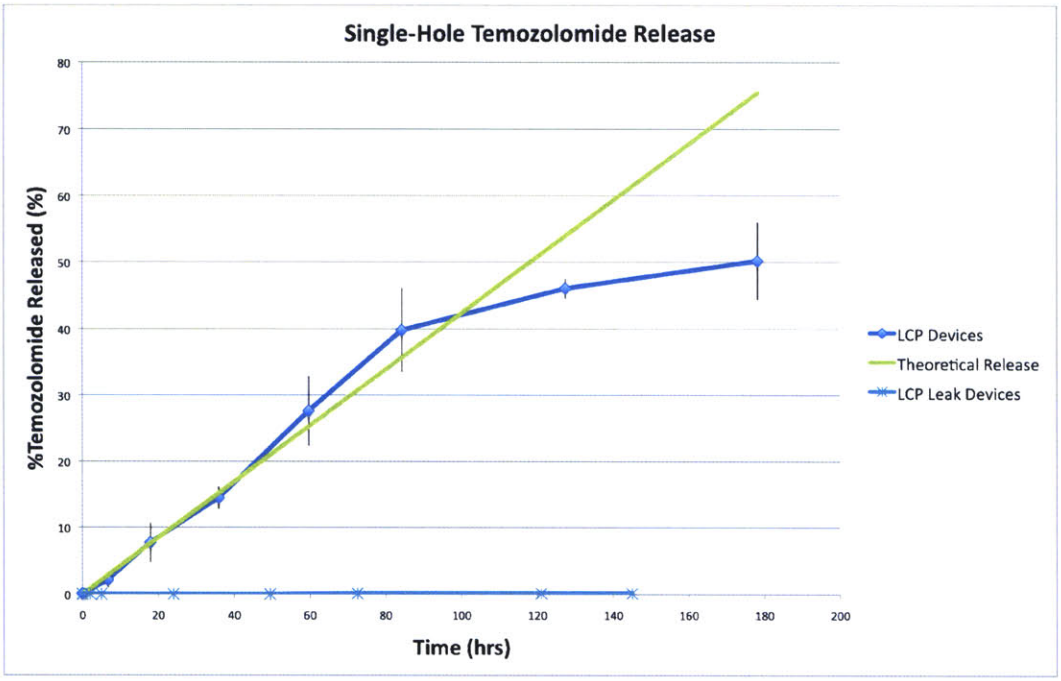

Figure 5-5: Single-Hole TMZ release into water

5.2.3 Multiple-Hole Devices

LCP devices with multiple drug release orifices were tested *in vitro* to examine the effect of increasing the number of release orifices on drug release rate. A theoretical release curve based on Fick's First Law of Diffusion was constructed for comparison with experimental drug release data. The mass flow rate calculated from Fick's 1st Law was 90 ug/hr. The number of devices for each group in this experiment was three. Results were reported as average values with standard deviations for each time point. The experimental release curves were in excellent agreement with the theoretical release curve. The experimental TMZ release rate during the first 100 hours of release was 88 ug/hr. At this time, 67% of the total 12mg was released. The release rate decreased after 100 hours, with a final drug release of 71% after 190 hours.

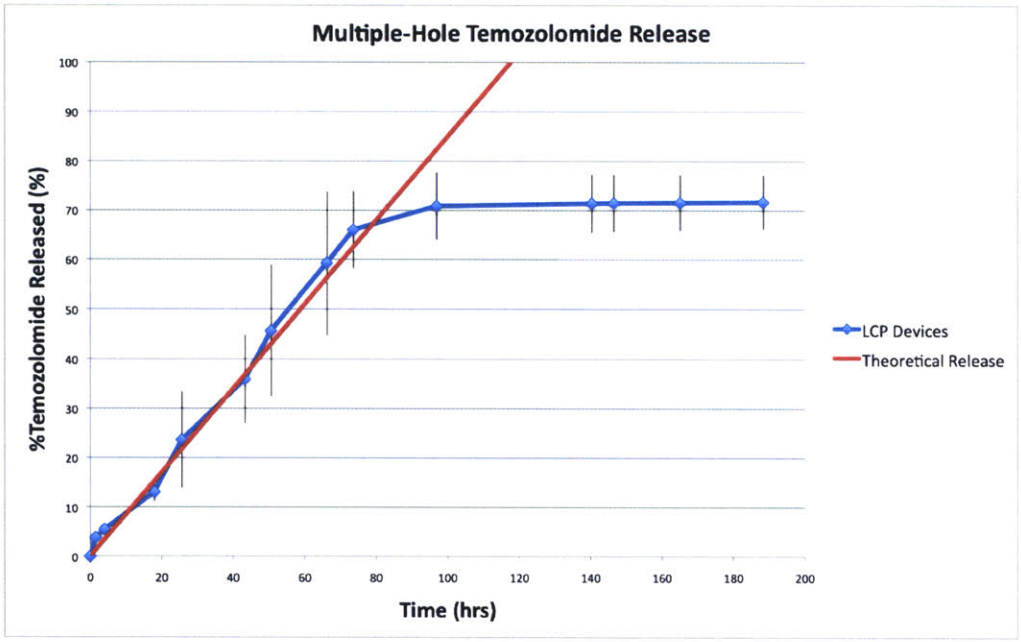

Figure 5-6: Multiple-Hole TMZ release into water

5.3 *In Vivo* Rodent Experiments

5.3.1 Fibrous Encapsulation

Fibrous encapsulation of foreign materials is a common response of the immune system. This response is induced in order to sequester potentially harmful materials from the rest of the body. The fibrous tissue commonly contains collagen, fibroblasts, macrophages, and other cells of the immune system. Explanted microcapsule devices were examined visually for fibrous capsule formation after animal death in all *in vivo* experiments. No fibrous tissue was found. The reasons and implications for this lack of fibrous tissue formation will be discussed in the following chapter.

5.3.2 Efficacy of Locally Delivered Temozolomide

Single-Hole Devices

In the initial *in vivo* rodent studies, the primary metric for drug delivery device efficacy was animal survival. Animals that received 9L tumor (control animals) and

blank LCP microcapsules had the highest rate of death and a median survival of 11 days for animals given blank LCP microcapsules. Control animals and animals in the blank PLLA device group died shortly after, with median survival times of 17 and 11 days, respectively. Rats given TMZ-loaded LCP and PLLA devices on day 5 after tumor implantation also showed high death rates and median respective survival times of 17 and 18 days.

Rats from the oral TMZ, TMZ wafer, and day zero TMZ microcapsule groups exhibited higher survival rates than the previously mentioned experimental groups. Animals given oral TMZ by gavage had a median survival time of 24 days. Increased rodent survival was achieved with the day zero TMZ-loaded LCP and PLLA groups, with median survival times of 31 and 50 days, respectively. The highest animal survival was found in the group that received two TMZ-impregnated polymer wafers on day five of tumor implantation. Animals in this group had a median survival time of 65 days.

Animals that survived 120 days or later were deemed long term survivors. There were three experimental groups in this initial *in vivo* study that contained long term survivors. These groups included 1) TMZ wafers, with four long term survivors. 2) LCP-TMZ day zero, with three long term survivors. 3) PLLA-TMZ day zero, with two long term survivors. No long term survivors were present in the group that received oral TMZ treatment, the current standard of care.

Statistical analysis of the survival data was performed in order to quantify the significance in animal survival between the control, oral, wafer, and LCP/PLLA TMZ day zero groups. Statistically significant differences were observed between control/wafer ($p<0.0001$), control/LCP-TMZ day zero ($p<0.0001$), oral/wafer ($p<0.0001$), and oral/LCP-TMZ day zero groups ($p=0.0187$). There was also statistical difference between the wafer/LCP-TMZ day zero ($p=0.0154$) and wafer/PLLA-TMZ day zero groups ($p=0.0004$), suggesting that the wafer devices performed better *in vivo* than the microcapsule devices. There was no statistically significant difference between the day zero TMZ-filled LCP and PLLA devices.

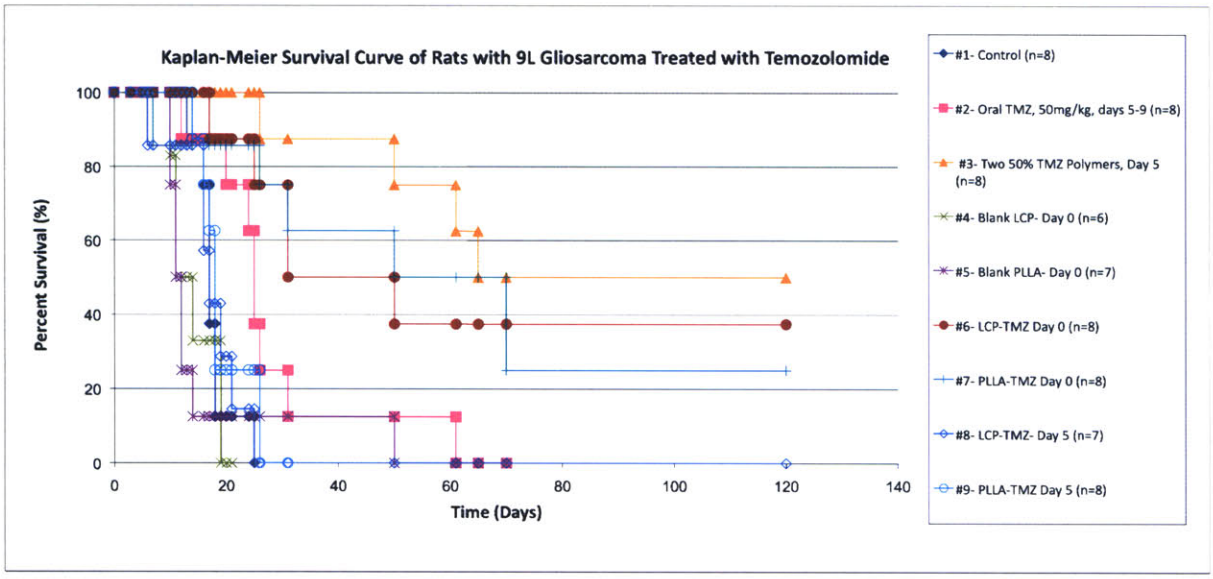

Figure 5-7: Localized TMZ Survival Experiment#1

Multiple-Hole Devices

The second *in vivo* TMZ experiment was performed in order to test the effectiveness of multiple orifice LCP microcapsule devices implanted on the day of tumor administration. The results of this study for control, oral, and blank devices were similar to the initial *in vivo* experiment. The median survival time for untreated control animals was 14 days. Oral gavage animals had a median survival time of 26 days, and day zero blank LCP animals had a median survival time of 13 days. Multiple orifice LCP devices showed a median survival time of 62 days. This survival advantage was two weeks greater than seen with single orifice LCP devices used in the first *in vivo* experiment. 37.5% of these animals were long term survivors.

Statistical analysis of the survival data was performed in order to quantify the significance in animal survival between the control, oral, and multiple hole LCP-TMZ day zero groups. Statistically significant differences were observed between control/oral ($p<0.0001$), control/LCP-TMZ day zero ($p<0.0001$), and oral/LCP-TMZ day zero groups ($p=0.0005$). The multiple-hole LCP devices have demonstrated improved rodent survival rates when compared with single-hole microcapsules and the current oral delivery standard of care.

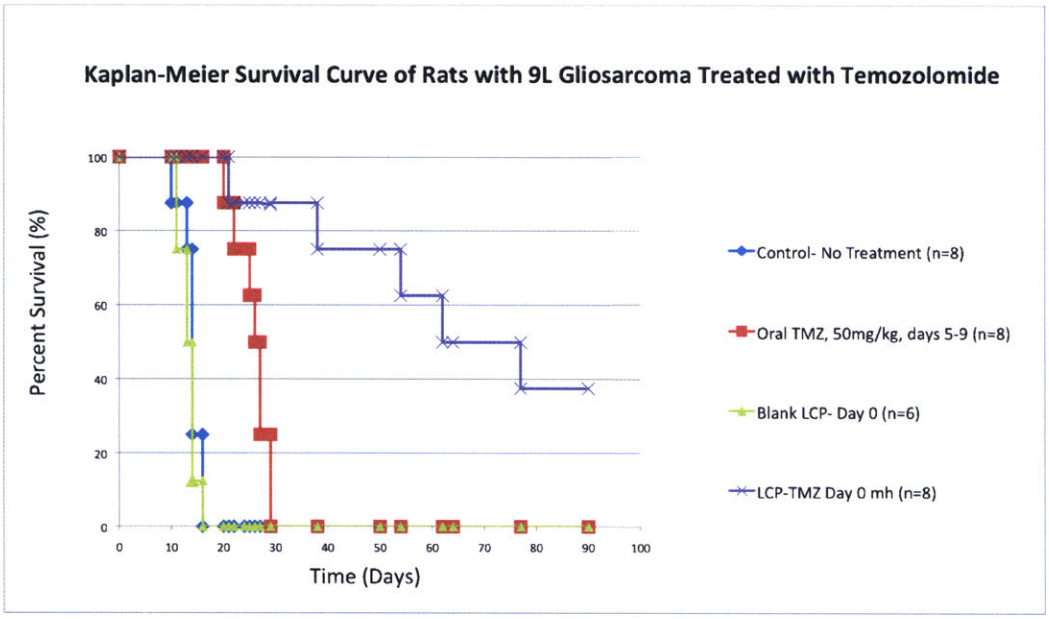

Figure 5-8: Localized TMZ Survival Experiment#2

5.4 *In Vitro* 9L Gliosarcoma Cell Culture

9L gliosarcoma cells were cultured *in vitro* and given varying concentrations of DOX to assess the sensitivity of these cells to DOX. Results showed that a minimum DOX concentration of 0.1ug/ml was capable of decreasing cell survival by 80% after 48 hours incubation. Drug concentrations lower than 0.1ug/ml showed varying amounts of activity against 9L cells, but the effect was not as dramatic as higher DOX concentrations. This MTT assay proved that the glioma model used in this work was sensitive to DOX.

5.5 *In Vitro* Doxorubicin Hydrochloride Drug Release Kinetics

A 1mg payload of DOX was loaded into single 180 μm diameter orifice LCP devices for *in vitro* drug release characterization. Control devices for leak tests with a payload of 1mg were also fabricated. The number of devices for each group in this experiment was two. Results were reported as average values with standard deviations for each

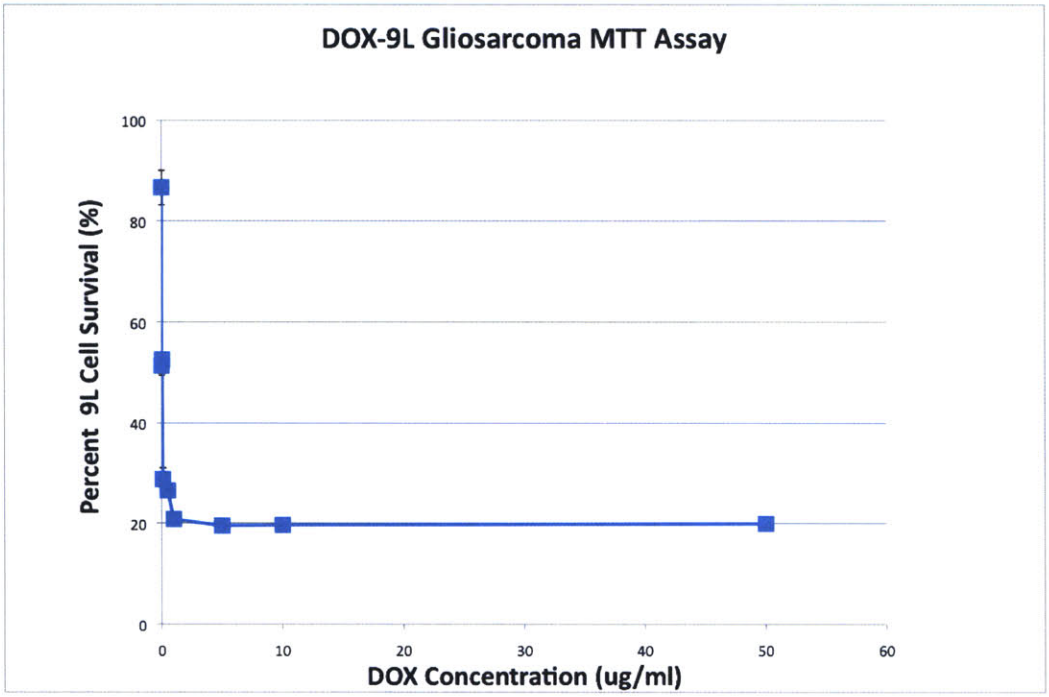

Figure 5-9: 9L-Doxorubicin MTT Assay

time point. The experimental DOX release rate during the first 100 hours of release (the linear region) was 5.6 ug/hr. At this time, 50% of the total 1mg was released. The release rate decreased after 100 hours, with a final drug release of 70% after 347 hours. Results from the drug leak experiments showed similar behavior as the TMZ leak devices. No drug was detected in the release bath after 350 hours.

5.6 Doxorubicin Hydrochloride Toxicity

In vivo doxorubicin hydrochloride toxicity studies were performed in order to test the feasibility of delivering the MTD local payload of 1mg DOX[16]. LCP microcapsule devices loaded with 1mg DOX were implanted intracranially in three rats at the beginning of the experiment. All animals survived for greater than 3 months and no toxic effects (neurological deficits, weight loss, failure to thrive, or wound healing problems) were observed.

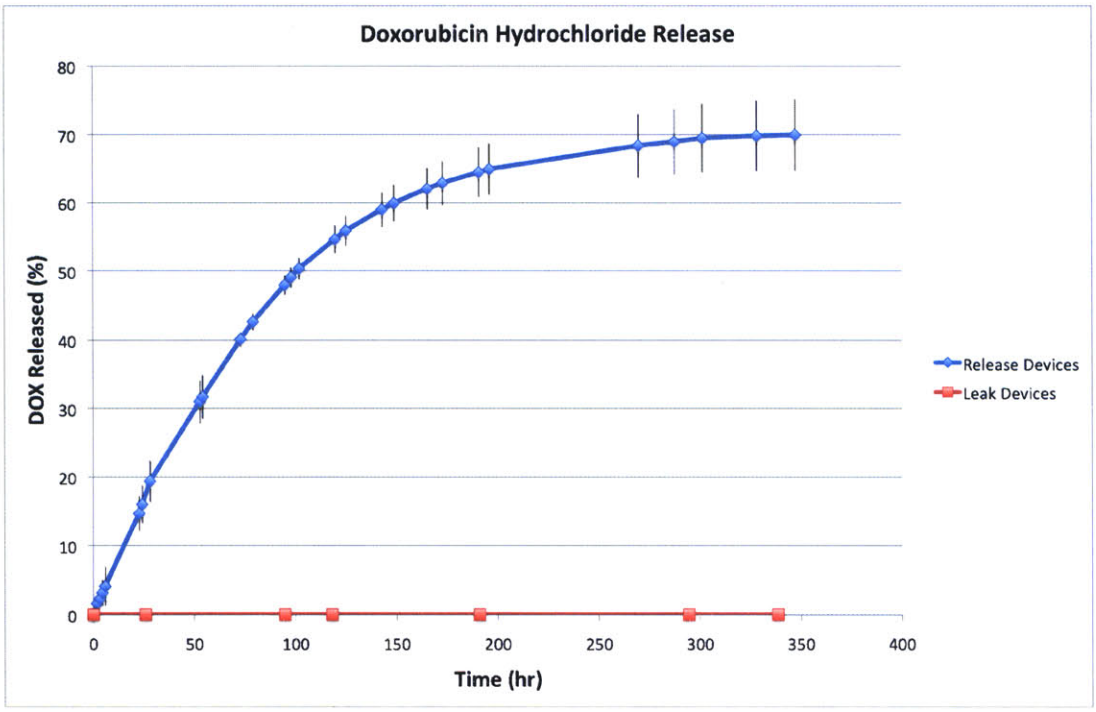

Figure 5-10: Release of doxorubicin hydrochloride into water

5.7 Immunohistochemical TUNEL Stain

TUNEL staining was conducted to assess the cytotoxicity of TMZ *in vivo*. Brain tissue samples were exposed to staining reagents and the number of TUNEL-positive cells in each sample was counted. Brain tissue sections were cut ipsilateral and contralateral to the location of the implanted devices in order to understand the significance of device location and drug distribution in the brain. Ipsilateral section cuts were made on the same side as the implanted device and contralateral section cuts were made on the opposite side of the brain. Results from the first *in vivo* survival study showed that the LCP-TMZ treatment group had higher ipsilateral TUNEL-positive cell counts than all other experimental groups. LCP-TMZ and TMZ-polymer wafer groups had statistically similar contralateral TUNEL-positive cell counts that were larger than control, blank LCP, and oral TMZ TUNEL-positive cell counts. Results from the second *in vivo* survival study also showed that the LCP-TMZ treatment group had higher ipsilateral TUNEL-positive cell counts than all other experimental groups.

Total TUNEL-positive cell counts (ipsilateral+contralateral) showed that tissue

samples from the LCP-TMZ treated rodent group from the first and second *in vivo* experiments had the largest number of TUNEL-positive cells. This number was higher than both the oral TMZ and TMZ-polymer composite wafer treatment groups. Control and blank LCP microcapsule groups showed the lowest total number of TUNEL-positive cells.

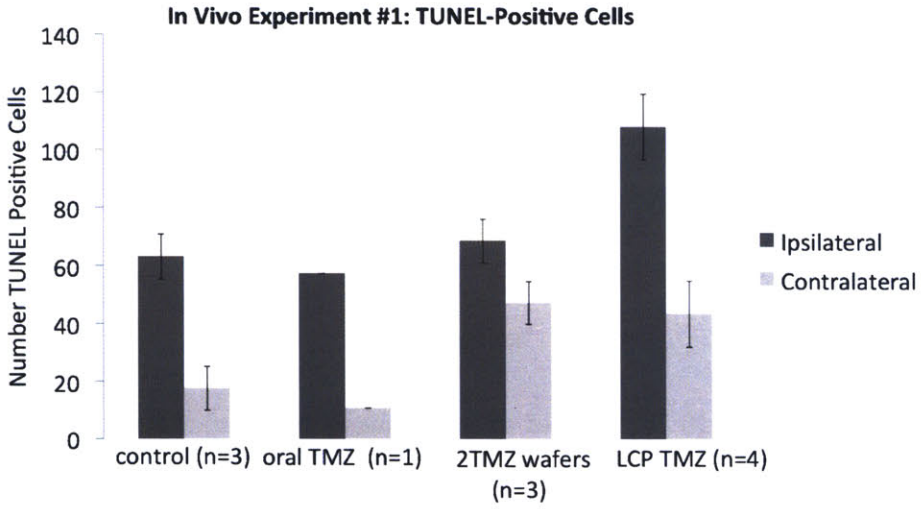

a.

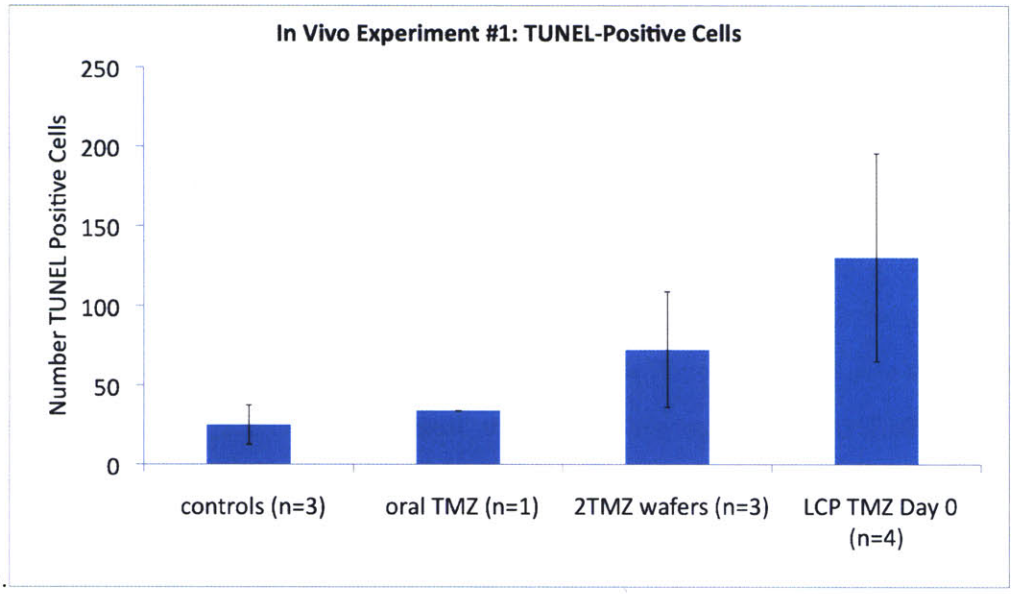

b.

Figure 5-11: *In Vivo* Experiment 1 TUNEL stain of rodent brain tissue a) Ipsilateral and contralateral brain section TUNEL stain b) Total (ipsilateral+contralateral) TUNEL-positive cell count

a.

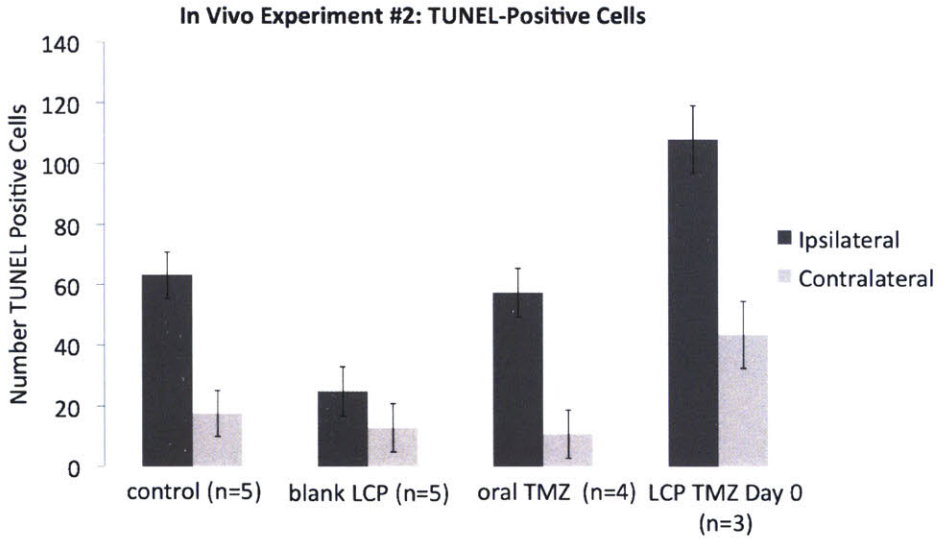

b.

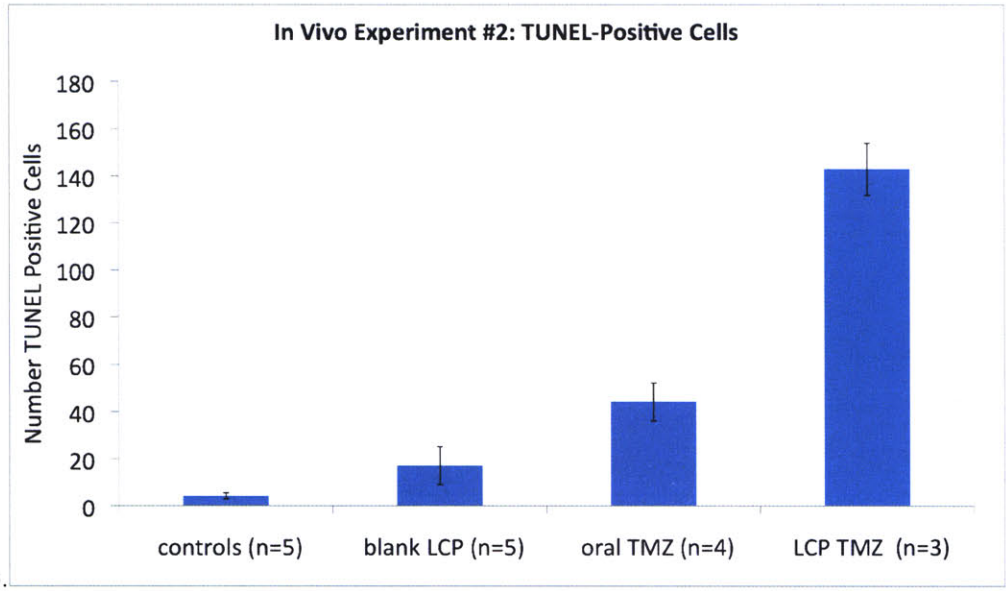

Figure 5-12: *In Vivo* Experiment 2 TUNEL stain of rodent brain tissue a) Ipsilateral and contralateral brain section TUNEL stain b) Total (ipsilateral+contralateral) TUNEL-positive cell count

Chapter 6

Discussion

6.1 Temozolomide Stability and Solubility

Temozolomide is known to be more stable and soluble under acidic conditions (pH<5) than in basic conditions (pH>7)[14]. Experimental results showed that TMZ was most stable in pH 7 water with a half-life of 99 hours (when compared to its stability in PBS and FBS). It is also important to note that the IV formulation of temozolomide developed by Schering-Plough is reconstituted with an aqueous buffer to form a solution with an acidic pH of 4 in order to increase the drug's stability in solution. The PBS used for TMZ stability experiments had a pH of 7.4 but TMZ showed a much shorter half-life of five hours in PBS than in water. Pre-clinical stability studies by Denny and Stevens have reported half-life values ranging from 1.24 to 1.38 hours for TMZ in aqueous phosphate buffer[48, 49]. Phosphate buffers used in those studies had a similar pH as the PBS used in this current work (pH=7.0-7.4). The different TMZ half-life values in solutions with similar pH values suggests that TMZ stability is not solely pH-dependent.

PBS contains inorganic salts that are used to maintain a constant pH and ion concentrations and osmolality that are tailored to match those of the human body. The PBS used in this work is formulated with monopotassium phosphate, sodium chloride, anhydrous disodium phosphate, and has an osmolality of 287 mOsm. It is not known what salt concentrations were used in the pre-clinical TMZ stability studies

performed by Denny and Stevens but ionic strength seems to play a role in decreasing the stability of TMZ in solution. The decreased stability of TMZ in biologically relevant solvents such as PBS and FBS in comparison to its stability in water is an important issue that directly affects the design of drug delivery microcapsules and requires strict analysis of the *in vitro* release kinetics of TMZ from these devices. Formulation of TMZ with an organic acid offers one way to increase the stability of drug in the microcapsule reservoir. This formulation method, however, is not without its own drawbacks, most important of which is the decrease in drug payload associated with co-formulation.

Experimental work performed in this thesis showed that TMZ was most soluble (11 mg/ml) in pH 3 buffer. It was thought that by formulating TMZ with an acidic molecule inside the microcapsule reservoir, we would be able to achieve greater drug stability and solubility. Greater solubility would allow for faster release kinetics for a given orifice size and higher concentrations of drug delivered to the tumor bed. The improved stability within the reservoir would improve the extent of release as less drug would degrade before diffusing out of the device. The maximum solubility only improved by approximately 30% from pH 7 water to its maximum at pH 3. Previous calculations showed that TMZ drug payload was one of the main limitations of the microcapsule delivery system, and this marginal improvement in solubility did not justify the loss of drug payload associated with co-formulation of TMZ with an organic acid.

6.2 *In Vitro* Temozolomide Drug Release Kinetics

6.2.1 Temozolomide-Polymer Composite Wafers

A total TMZ payload of 3.75mg was released from polymer wafers into water after 62 hours. Drug release began to plateau after this time period. Similar drug release behavior was seen by Brem et al. The total TMZ release from polymer-drug composite wafers measured by the Brem group was 3.5mg[30]. The discrepancies in the drug

release data between our group and Brem's may be due to slight variations in total drug payloads (the polymer wafers are loaded 50% (w/w) with TMZ by the solvent method[30]) between wafers. The solvent method of loading drug into polymer composite devices requires solutionization of TMZ. This can cause drug degradation before TMZ is loaded into the polymer matrix, effectively reducing the final drug payload. The detection methods between the two experiments were also different, the Brem group used radioactive liquid scintillation counting (LSC) to quantify tritium-labeled TMZ, and our group used HPLC for non-radioactive labeled TMZ. The total amount of drug released by the end of each experiment was similar despite the differences in experimental setup and quantitative analysis methods.

6.2.2 Temozolomide-loaded Microcapsule Devices

Single and multiple-hole drug delivery microcapsules showed similar *in vitro* drug release behavior. Both types of devices exhibited close agreement with theoretical mass flow rate calculations for the first 100 hours of drug release. The release rates of the single and multiple-hole microcapsules began to plateau after this time. This plateau is due to a decrease in the chemical driving force for diffusion and drug degradation. Our use of Fick's First Law of Diffusion assumes that the microcapsule reservoir is completely saturated with drug and the outside environment is at sink conditions throughout the entire period of drug release. This allows for simplification of the diffusion equation (a linear concentration gradient that does not change with time) that still captures the majority of the experimentally-determined drug release behavior. The actual behavior of TMZ over the entire course of drug release is not as straightforward. The driving force for diffusion decreases as drug is released from the microcapsule reservoir because the reservoir is no longer completely saturated with drug. The concentration profile between the reservoir and outside environment begins to approach the same value as drug is released, and the mass flow rate across the device orifice decreases. This results in slower drug diffusion than predicted theoretically from Fick's First Law. One way to express this change in drug concentration with time is to use Fick's Second Law of Diffusion. This equation takes into account changes

in drug concentration over space and time. Its application to this work is made more complex than Fick's First Law due to the fact that specific experimentally determined boundary conditions must be set up in order to solve the equation. Future work will study the applicability of Fick's Second Law of Diffusion to the release kinetics of these drug delivery microcapsules.

The stability of TMZ also has a profound impact on the *in vitro* release kinetics of drug delivery microcapsules. TMZ is a prodrug that quickly degrades into the bioactive MTIC molecule under basic conditions and in high ionic strength solvents. *In vitro* release profiles of TMZ into water from microcapsule devices highlight the importance of specifying the environment that the drug of interest is released into. The half-life of TMZ in water is considerably greater than its half-life in PBS, FBS, and *in vivo*, as mentioned previously. This accounts for the close agreement with theory that is seen during the first 100 hours of the TMZ-water release profiles. The current HPLC method is sensitive to TMZ and is unable to detect MTIC molecules in solution. This is shown by the difference between theoretical release kinetics, which assume only one type of molecule in solution (TMZ), and experimental release of TMZ from our devices over time periods greater than 100 hours. Degradation of TMZ due to its instability in solution accounts for the plateau in drug release over long periods of time and also explains why 100% drug release is not seen experimentally. Knowledge of the stability characteristics of TMZ in approximate *in vivo* conditions is an excellent asset in interpreting *in vitro* results and designing drug delivery devices for *in vivo* studies. Future work employing the use of HPLC/MS systems along with improved analysis methods that are able to detect MTIC will allow us to characterize the release of both TMZ and MTIC from these devices.

6.3 *In Vivo* Rodent Experiments

6.3.1 Fibrous Encapsulation

Empty PLLA and LCP microcapsule devices were implanted in the flank and intracranially in Fischer 344 rats. Devices were implanted for a total of 30 days. Visual inspection confirmed that fibrous tissue was present on devices implanted in the flank but not on devices implanted in the brain. Previous work by Lillehei et al. also showed that PLLA drug delivery devices appeared to be inert when implanted intracranially. This group performed histological analysis on the brain tissue surrounding the polymer implants in addition to visual inspection of the explanted polymer. They found that histologically, no macrophages, mononuclear cells, or significant histiocytic response was present 40 days after polymer implantation[50]. A mild foreign body reaction surrounding the site of the polymer was noted, but no fibrous tissue growth was present intracranially. Our results agree with those found in the Lillehei study, but further histological work needs to be conducted to ascertain the reasons for the fibrous device encapsulation that occurs in the flank but not in the brain.

The apparent lack of intracranial immune response to the microcapsule drug delivery system is important for two reasons: 1) It proves that the polymers used for the microcapsule housing are non-toxic and biocompatible. 2) The lack of fibrous capsule formation keeps the drug-eluting orifices from being occluded by tissue, ensuring drug release *in vivo*. Long-term *in vivo* efficacy studies (120 days) also confirmed a lack of fibrous tissue formation. This suggests that the polymers used for fabrication of these microcapsule devices are biocompatible and suitable for intracranial rodent implantation.

6.3.2 Efficacy of Locally Delivered Temozolomide

The *in vivo* efficacy of localized TMZ therapy was investigated against the 9L glioma model in rodents. Results showed that the implantation of two 50% (w/w) TMZ-polymer wafers prolonged animal survival the longest in comparison to all experi-

mental groups. These devices were implanted five days after tumor implantation. Microcapsule devices (single and multiple-orifice) implanted on the same day as 9L tumor showed the second-best survival benefit in tumor-challenged rats. Both localized drug delivery systems out-performed Temodar®, the current standard of care for GBM treatment.

Polymer-drug composite wafers are capable of multi-directional drug diffusion because the entire device surface is exposed to the tumor bed and is able to release drug. Microcapsule devices, on the other hand, are only able to release drug from either one orifice or five orifices. Multiple-orifice microcapsules extended median animal survival by two weeks when compared with single-orifice devices. The faster drug release kinetics provided by the multiple-orifice microcapsules (proven by *in vitro* drug release experiments) deliver a larger drug payload to the tumor than single-orifice devices over a shorter period of time. This relatively quick release is important to maintaining the potency of the inherently unstable TMZ molecule. Additional release orifices can be fabricated in microcapsule reservoirs in order to approach the truly multi-directional drug release achieved by the wafer system.

The device implantation procedure also has important ramifications on the efficacy of localized treatment. The microcapsule dimensions were chosen for delivery of a large drug payload from a device that is still small enough for implantation in the rodent brain cavity. The tight dimensional tolerances between the rodent skull and the microcapsule device along with the introduction of a growing 9L tumor mass causes brain damage due to increased intracranial pressure (mass effect). This increase in pressure is a common manifestation in GBM patients and is one of the primary reasons for tumor resection surgery. The detrimental effect of increased intracranial pressure is shown by the relatively quick animal deaths present in the blank microcapsule device groups.

The effect of decreased "free volume" between the microcapsule drug release orifice and brain tissue due to growing tumor also explains why multiple-orifice devices performed better than single-orifice devices, and why day zero microcapsule devices performed better than day five microcapsules devices. The hypothesis is that grow-

ing tumor causes increased intracranial pressure, as noted in the previous paragraph, and this tissue mass also occludes the drug-releasing orifice in single-hole devices. This occlusion occurs because the devices are implanted with the orifice facing the tumor. Multiple-orifice devices and polymer wafers are capable of multi-directional drug release that is able to avoid the occlusion caused by the growing tissue mass. Explanted single-orifice devices were found to have residual TMZ left in the reservoir and multi-orifice devices were completely empty. Day zero microcapsules out-performed day five devices because the tumor mass on day zero was not as large as the tumor mass present on day five. The efficacy of localized drug delivery devices in this work is directly related to their size and ability for multi-directional drug release. The progressive improvement in animal survival from single-orifice microcapsules to multiple-orifice microcapsules to polymer wafers confirms this. It may also be beneficial to move to larger animal models where there is more intracranial space for microcapsule implantation and lower probability of orifice occlusion.

The need for delivery of high drug concentrations to GBM locally was the motivating factor of this work, and the PLLA and LCP microcapsule devices developed by our group look to improve upon the successes of the Gliadel® wafer and the polymer-matrix composite wafers fabricated by the Brem group at Johns Hopkins University[30][8]. The microcapsule system delivers more than twice the drug payload as the TMZ-polymer matrix wafers in a similar volume that is suitable for intracranial implantation. Microcapsule devices are also capable of delivering solid or liquid drug formulations, an ability that polymer-composite wafer systems do not currently possess. This allows for highly versatile and tunable drug delivery with the possibility of delivering a wide range of therapeutic compounds to brain tumors and other human diseases.

6.4 Immunohistochemical TUNEL Stain

Animals treated with TMZ showed the largest number of TUNEL-positive cells when compared to both control groups (tumor only and blank LCP). This behavior is to be

expected because TMZ is known to cause single and double stranded DNA breaks, or "nicks," and animals that were not exposed to TMZ (both control groups) showed very low levels of TUNEL-positive cells. The relatively low TUNEL staining present in the oral TMZ group is probably due to low partitioning of TMZ from systemic circulation to the brain, with only an estimated 35% of the oral TMZ dosage reaching the brain. The higher drug payload in the LCP microcapsule devices (12mg) may explain why more TUNEL-positive cells were found in this group versus the TMZ wafer group.

One interesting observation from the TUNEL stain experiment is that the results for LCP-TMZ microcapsules versus polymer wafers do not correlate with the animal survival studies. The animals in the LCP-TMZ group had a higher overall number of TUNEL-positive cells than the TMZ-polymer wafer group, but longer survival was observed in the wafer group. One possible reason for this increase in survival may be due to insufficient tumor targeting. The cytotoxicity of TMZ is non-specific to cancer cells due to the fact that all cells are affected by DNA damage induced by the drug. Localized delivery of TMZ increases the exposure of tumor cells to drug while avoiding the cytotoxic effects imposed on normal healthy cells by TMZ. The total number of TUNEL-positive cells is certainly higher in the LCP-TMZ group than in the wafer group, but in addition to damaged 9L cells, these numbers include healthy brain cells that have been damaged by TMZ and are also undergoing apoptosis. The overall effect is that more cells (healthy and cancerous) may be damaged in the LCP-TMZ group, causing brain/tumor damage and death.

6.5 Doxorubicin Hydrochloride Studies

Doxorubicin hydrochloride was chosen for experimentation based on its unacceptable side-effects when administered systemically (congestive heart failure in 20% of patients), proven activity against GBM, and significantly reduced total local drug payload in comparison to TMZ. Initial DOX studies included drug efficacy studies against 9L glioma cells *in vitro*, DOX release studies from microcapsules *in vitro*, and DOX toxicity studies in Fischer 344 rodents. Our *in vitro* efficacy experiments con-

firmed that 9L glioma cells were sensitive to DOX at low concentrations of 0.1ug/ml. This allowed us to move forward to develop microcapsules that were capable of delivering DOX locally *in vivo*. *In vitro* drug release kinetics and *in vivo* toxicity studies suggested that local delivery of 1mg DOX over two weeks was safe and well-tolerated in our rodent model. Future studies will examine the efficacy of localized DOX delivery in comparison with systemic administration of Doxil®, the current standard of care formulation of DOX.

Chapter 7

Conclusions and Future Work

The work conducted in this thesis has demonstrated that polymer microcapsule devices are capable of releasing chemotherapeutic molecules *in vitro* at rates similar to theoretical values calculated from Fick's First Law of Diffusion. The polymers used in the manufacture of these devices are both biocompatible (LCP and PLLA) and biodegradable (PLLA) when implanted intracranially in a rodent animal model. Molecular histochemical analysis and MTT assay confirms the ability of drugs used in this thesis to cause cytotoxic DNA damage in cell nuclei. I have also shown that implantable drug delivery devices are capable of significantly prolonging survival in 9L glioma-challenged rodents in comparison with systemic delivery methods. Issues related to unattainable drug payloads needed for complete TMZ therapy led to the selection of doxorubicin as the second chemotherapeutic of interest. *In vitro* release experiments proved that microcapsule devices are able to release DOX payloads reliably. Further *in vitro* testing of these devices along with *in vivo* DOX dose escalation trials will allow for future *in vivo* rodent efficacy studies. Work is ongoing to produce a syringe injectable multiple reservoir version with the capability of releasing a range of therapeutic compounds in solid or liquid formulations. We have chosen to focus on treatment of glioblastoma multiforme in this work but through knowledge of clinically relevant dosing schedules, chemotherapeutic solubility and stability, and with minor changes in device orifice diameter, it will be possible to use these drug delivery microcapsules to treat a range of human diseases.

Bibliography

[1] M. Prados and V. Levin, "Biology and treatment of malignant glioma.," in *Seminars in oncology*, vol. 27, p. 1, 2000.

[2] G. Kitange, J. Smith, and R. Jenkins, "Genetic alterations and chemotherapeutic response in human diffuse gliomas," *Expert Review of Anticancer Therapy*, vol. 1, no. 4, pp. 595–605, 2001.

[3] P. Kleihues, D. Louis, B. Scheithauer, L. Rorke, G. Reifenberger, P. Burger, and W. Cavenee, "The who classification of tumors of the nervous system," *Journal of Neuropathology & Experimental Neurology*, vol. 61, no. 3, p. 215, 2002.

[4] P. Giglio, "Chemotherapy for glioblastoma: Past, present, and future," *Glioblastoma:*, pp. 203–216.

[5] K. Jellinger, "Glioblastoma multiforme: morphology and biology," *Acta neurochirurgica*, vol. 42, no. 1, pp. 5–32, 1978.

[6] L. Hou, A. Veeravagu, A. Hsu, and V. Tse, "Recurrent glioblastoma multiforme: a review of natural history and management options," *Neurosurgical Focus*, vol. 20, no. 4, p. 3, 2006.

[7] K. Kelly, J. Kirkwood, and D. Kapp, "Glioblastoma multiforme: pathology, natural history and treatment.," *Cancer treatment reviews*, vol. 11, no. 1, p. 1, 1984.

[8] D. Bota, A. Desjardins, J. Quinn, M. Affronti, and H. Friedman, "Interstitial chemotherapy with biodegradable bcnu (gliadel®) wafers in the treatment of

malignant gliomas," *Therapeutics and Clinical Risk Management*, vol. 3, no. 5, p. 707, 2007.

[9] S. Agarwala and J. Kirkwood, "Temozolomide, a novel alkylating agent with activity in the central nervous system, may improve the treatment of advanced metastatic melanoma," *The Oncologist*, vol. 5, no. 2, p. 144, 2000.

[10] C. Wang, J. Li, C. Teo, and T. Lee, "The delivery of bcnu to brain tumors," *Journal of Controlled Release*, vol. 61, no. 1-2, pp. 21–41, 1999.

[11] G. Kim, B. Tyler, M. Tupper, J. Karp, R. Langer, H. Brem, and M. Cima, "Resorbable polymer microchips releasing bcnu inhibit tumor growth in the rat 9l flank model," *Journal of Controlled Release*, vol. 123, no. 2, pp. 172–178, 2007.

[12] C. Guerin, A. Olivi, J. Weingart, H. Lawson, and H. Brem, "Recent advances in brain tumor therapy: local intracerebral drug delivery by polymers," *Investigational new drugs*, vol. 22, no. 1, pp. 27–37, 2004.

[13] H. Zhang and S. Gao, "Temozolomide/plga microparticles and antitumor activity against glioma c6 cancer cells in vitro," *International journal of pharmaceutics*, vol. 329, no. 1-2, pp. 122–128, 2007.

[14] E. Newlands, M. Stevens, S. Wedge, R. Wheelhouse, and C. Brock, "Temozolomide: a review of its discovery, chemical properties, pre-clinical development and clinical trials* 1," *Cancer treatment reviews*, vol. 23, no. 1, pp. 35-61, 1997.

[15] R. Stupp, W. Mason, M. van den Bent, M. Weller, B. Fisher, M. Taphoorn, K. Belanger, A. Brandes, C. Marosi, U. Bogdahn, *et al.*, "Radiotherapy plus concomitant and adjuvant temozolomide for glioblastoma," *The New England journal of medicine*, vol. 352, no. 10, p. 987, 2005.

[16] M. LESNIAK, U. UPADHYAY, R. GOODWIN, B. TYLER, and H. BREM, "Local delivery of doxorubicin for the treatment of malignant brain tumors in rats," *Anticancer research*, vol. 25, no. 6B, p. 3825, 2005.

[17] F. Arcamone, G. Cassinelli, G. Fantini, A. Grein, P. Orezzi, C. Pol, and C. Spalla, "14-hydroxydaunomycin, a new antitumor antibiotic from streptomyces peucetius var. caesius," *Biotechnol. Bioeng*, vol. 11, pp. 1101–1110, 1969.

[18] K. Wallace, "Doxorubicin-induced cardiac mitochondrionopathy," *Pharmacology & toxicology*, vol. 93, no. 3, pp. 105–115, 2003.

[19] B. Diez, P. Statkevich, Y. Zhu, M. Abutarif, F. Xuan, B. Kantesaria, D. Cutler, M. Cantillon, M. Schwarz, M. Pallotta, *et al.*, "Evaluation of the exposure equivalence of oral versus intravenous temozolomide," *Cancer Chemotherapy and Pharmacology*, pp. 1–8.

[20] A. Sawyer, J. Piepmeier, and W. Saltzman, "Cancer issue: New methods for direct delivery of chemotherapy for treating brain tumors," *The Yale Journal of Biology and Medicine*, vol. 79, no. 3-4, p. 141, 2006.

[21] R. Raghavan, M. Brady, M. Rodríguez-Ponce, A. Hartlep, C. Pedain, and J. Sampson, "Convection-enhanced delivery of therapeutics for brain disease, and its optimization," *Neurosurg Focus*, vol. 20, no. 4, p. E12, 2006.

[22] H. Brem and P. Gabikian, "Biodegradable polymer implants to treat brain tumors," *Journal of Controlled Release*, vol. 74, no. 1-3, pp. 63–67, 2001.

[23] J. Heller, "Patient-friendly bioerodible drug delivery systems," *Journal of Controlled Release*, vol. 133, no. 2, pp. 88–89, 2009.

[24] D. Arifin, K. Lee, C. Wang, and K. Smith, "Role of convective flow in carmustine delivery to a brain tumor," *Pharmaceutical Research*, vol. 26, no. 10, pp. 2289–2302, 2009.

[25] T. Siegal, A. Horowitz, and A. Gabizon, "Doxorubicin encapsulated in sterically stabilized liposomes for the treatment of a brain tumor model: biodistribution and therapeutic efficacy," *Journal of neurosurgery*, vol. 83, no. 6, pp. 1029–1037, 1995.

[26] T. Kikuchi, R. Saito, S. Sugiyama, Y. Yamashita, T. Kumabe, M. Krauze, K. Bankiewicz, and T. Tominaga, "Convection-enhanced delivery of polyethylene glycol-coated liposomal doxorubicin: characterization and efficacy in rat intracranial glioma models," *Journal of Neurosurgery*, vol. 109, no. 5, pp. 867–873, 2008.

[27] M. Hart, R. Grant, R. Garside, G. Rogers, M. Somerville, and K. Stein, "Chemotherapeutic wafers for high grade glioma.," *Cochrane database of systematic reviews (Online)*, no. 3, 2008.

[28] P. Hiemenz and R. Rajagopalan, *Principles of colloid and surface chemistry.* CRC, 1997.

[29] A. Tolcher, S. Gerson, L. Denis, C. Geyer, L. Hammond, A. Patnaik, A. Goetz, G. Schwartz, T. Edwards, L. Reyderman, *et al.*, "Marked inactivation of o6-alkylguanine-dna alkyltransferase activity with protracted temozolomide schedules," *British journal of cancer*, vol. 88, no. 7, p. 1004, 2003.

[30] S. Brem, B. Tyler, K. Li, G. Pradilla, F. Legnani, J. Caplan, and H. Brem, "Local delivery of temozolomide by biodegradable polymers is superior to oral administration in a rodent glioma model," *Cancer chemotherapy and pharmacology*, vol. 60, no. 5, pp. 643–650, 2007.

[31] W. Consultation, "Obesity: preventing and managing the global epidemic," *World Health Organization Technical Report Series*, vol. 894, 2000.

[32] B. Ebert, E. Niemierko, K. Shaffer, and R. Salgia, "Use of temozolomide with other cytotoxic chemotherapy in the treatment of patients with recurrent brain metastases from lung cancer," *The Oncologist*, vol. 8, no. 1, p. 69, 2003.

[33] R. Stupp, P. Dietrich, S. Kraljevic, A. Pica, I. Maillard, P. Maeder, R. Meuli, R. Janzer, G. Pizzolato, R. Miralbell, *et al.*, "Promising survival for patients with newly diagnosed glioblastoma multiforme treated with concomitant radia-

tion plus temozolomide followed by adjuvant temozolomide," *Journal of Clinical Oncology*, vol. 20, no. 5, p. 1375, 2002.

[34] S. Voulgaris, M. Partheni, M. Karamouzis, P. Dimopoulos, N. Papadakis, and H. Kalofonos, "Intratumoral doxorubicin in patients with malignant brain gliomas," *American journal of clinical oncology*, vol. 25, no. 1, p. 60, 2002.

[35] K. Uhrich, S. Cannizzaro, R. Langer, and K. Shakesheff, "Polymeric systems for controlled drug release," *Chem. Rev*, vol. 99, no. 11, pp. 3181–3198, 1999.

[36] A. Grayson, I. Choi, B. Tyler, P. Wang, H. Brem, M. Cima, and R. Langer, "Multi-pulse drug delivery from a resorbable polymeric microchip device," *Nature Materials*, vol. 2, no. 11, pp. 767–772, 2003.

[37] S. Kaihara, S. Matsumura, A. Mikos, and J. Fisher, "Synthesis of poly (l-lactide) and polyglycolide by ring-opening polymerization," *Nature Protocols*, vol. 2, no. 11, pp. 2767–2771, 2007.

[38] G. Odian, *Principles of polymerization.* John Wiley and Sons, 2004.

[39] X. Wang, J. Engel, and C. Liu, "Liquid crystal polymer for mems: processes and applications," *Journal of Micromechanics and Microengineering*, vol. 13, pp. 628–633, 2003.

[40] R. Lusignea, "Liquid crystal polymers: new barrier materials for packaging," *Packaging Technology and Engineering*, vol. 6, pp. 38–43, 1997.

[41] R. Barth, "Rat brain tumor models in experimental neuro-oncology: the 9l, c6, t9, f98, rg2 (d74), rt-2 and cns-1 gliomas," *Journal of neuro-oncology*, vol. 36, no. 1, pp. 91–102, 1998.

[42] H. Kim, C. Lin, D. Parker, J. Veals, J. Lim, P. Likhari, P. Statkevich, A. Marco, and A. Nomeir, "High-performance liquid chromatographic determination and stability of 5-(3-methyltriazen-1-yl)-imidazo-4-carboximide, the biologically active product of the antitumor agent temozolomide, in human plasma," *Journal*

of Chromatography B: Biomedical Sciences and Applications, vol. 703, no. 1-2, pp. 225–233, 1997.

[43] A. Gabizon, R. Catane, B. Uziely, B. Kaufman, T. Safra, R. Cohen, F. Martin, A. Huang, and Y. Barenholz, "Prolonged circulation time and enhanced accumulation in malignant exudates of doxorubicin encapsulated in polyethylene-glycol coated liposomes," *Cancer Research*, vol. 54, no. 4, p. 987, 1994.

[44] R. Tamargo, J. Myseros, J. Epstein, M. Yang, M. Chasin, and H. Brem, "Interstitial chemotherapy of the 9l gliosarcoma: controlled release polymers for drug delivery in the brain," *Cancer research*, vol. 53, no. 2, p. 329, 1993.

[45] Y. Gavrieli, Y. Sherman, and S. Ben-Sasson, "Identification of programmed cell death in situ via specific labeling of nuclear dna fragmentation," *Journal of Cell Biology*, vol. 119, no. 3, p. 493, 1992.

[46] V. Heatwole, "Tunel assay for apoptotic cells," *METHODS IN MOLECULAR BIOLOGY-CLIFTON THEN TOTOWA-*, vol. 115, pp. 141–148, 1999.

[47] Q. Zhou, P. Guo, X. Wang, S. Nuthalapati, and J. Gallo, "Preclinical pharmacokinetic and pharmacodynamic evaluation of metronomic and conventional temozolomide dosing regimens," *Journal of Pharmacology and Experimental Therapeutics*, vol. 321, no. 1, p. 265, 2007.

[48] B. Denny, R. Wheelhouse, M. Stevens, L. Tsang, and J. Slack, "Nmr and molecular modeling investigation of the mechanism of activation of the antitumor drug temozolomide and its interaction with dna," *Biochemistry*, vol. 33, no. 31, pp. 9045–9051, 1994.

[49] M. Stevens, J. Hickman, S. Langdon, D. Chubb, L. Vickers, R. Stone, G. Baig, C. Goddard, N. Gibson, J. Slack, *et al.*, "Antitumor activity and pharmacokinetics in mice of 8-carbamoyl-3-methyl-imidazo [5, 1-d]-1, 2, 3, 5-tetrazin-4 (3h)-one (ccrg 81045; m & b 39831), a novel drug with potential as an alternative to dacarbazine," *Cancer research*, vol. 47, no. 22, p. 5846, 1987.

[50] K. Lillehei, Q. Kong, S. Withrow, and B. Kleinschmidt-DeMasters, "Efficacy of intralesionally administered cisplatin-impregnated biodegradable polymer for the treatment of 9l gliosarcoma in the rat," *Neurosurgery*, vol. 39, no. 6, p. 1191, 1996.